


2000

# A new soil performance classification system and utilizations of fly ash as a construction material

David Joshua White  
*Iowa State University*

Follow this and additional works at: <https://lib.dr.iastate.edu/rtd>

 Part of the [Civil Engineering Commons](#), and the [Materials Science and Engineering Commons](#)

## Recommended Citation

White, David Joshua, "A new soil performance classification system and utilizations of fly ash as a construction material " (2000).  
*Retrospective Theses and Dissertations*. 12373.  
<https://lib.dr.iastate.edu/rtd/12373>

This Dissertation is brought to you for free and open access by the Iowa State University Capstones, Theses and Dissertations at Iowa State University Digital Repository. It has been accepted for inclusion in Retrospective Theses and Dissertations by an authorized administrator of Iowa State University Digital Repository. For more information, please contact [digirep@iastate.edu](mailto:digirep@iastate.edu).

## **INFORMATION TO USERS**

**This manuscript has been reproduced from the microfilm master. UMI films the text directly from the original or copy submitted. Thus, some thesis and dissertation copies are in typewriter face, while others may be from any type of computer printer.**

**The quality of this reproduction is dependent upon the quality of the copy submitted. Broken or indistinct print, colored or poor quality illustrations and photographs, print bleedthrough, substandard margins, and improper alignment can adversely affect reproduction.**

**In the unlikely event that the author did not send UMI a complete manuscript and there are missing pages, these will be noted. Also, if unauthorized copyright material had to be removed, a note will indicate the deletion.**

**Oversize materials (e.g., maps, drawings, charts) are reproduced by sectioning the original, beginning at the upper left-hand corner and continuing from left to right in equal sections with small overlaps.**

**Photographs included in the original manuscript have been reproduced xerographically in this copy. Higher quality 6" x 9" black and white photographic prints are available for any photographs or illustrations appearing in this copy for an additional charge. Contact UMI directly to order.**

**Bell & Howell Information and Learning  
300 North Zeeb Road, Ann Arbor, MI 48106-1346 USA  
800-521-0600**

**UMI<sup>®</sup>**



A new soil performance classification system and  
utilizations of fly ash as a construction material

by

David Joshua White

A dissertation submitted to the graduate faculty  
in partial fulfillment of the requirements for the degree of  
DOCTOR OF PHILOSOPHY

Major: Civil Engineering (Geotechnical Engineering and Civil Engineering Materials)

Major Professors: John M. Pitt and Kenneth L. Bergeson

Iowa State University

Ames, Iowa

2000

**UMI Number: 9990500**

**UMI<sup>®</sup>**

---

**UMI Microform 9990500**

**Copyright 2001 by Bell & Howell Information and Learning Company.**

**All rights reserved. This microform edition is protected against  
unauthorized copying under Title 17, United States Code.**

---

**Bell & Howell Information and Learning Company  
300 North Zeeb Road  
P.O. Box 1346  
Ann Arbor, MI 48106-1346**

**Graduate College**  
**Iowa State University**

This is to certify that the Doctoral dissertation of  
**David Joshua White**  
has met the dissertation requirements of Iowa State University

Signature was redacted for privacy.

**Co-major Professor**

Signature was redacted for privacy.

**Co-major Professor**

Signature was redacted for privacy.

**For the Major Program**

Signature was redacted for privacy.

**For the Graduate College**

## TABLE OF CONTENTS

	Page
LIST OF FIGURES	v
LIST OF TABLES	vii
CHAPTER I. GENERAL INTRODUCTION	1
Dissertation Organization	1
Long Term Strength and Durability of Hydrated Fly Ash Road Bases	2
Microstructure of Composite Material from High-Lime Fly Ash and RPET	3
Empirical Performance Classification for Cohesive Embankment Soils	5
CHAPTER II. LONG TERM STRENGTH AND DURABILITY OF HYDRATED FLY ASH ROAD BASES	7
Abstract	7
Introduction	8
Material Properties	10
Reclaimed Hydrated Fly Ash (HFA)	10
Cement Kiln Dust (CKD)	10
Atmospheric Fluidized Bed Combustion (AFBC) Residue	11
Laboratory Testing	12
Moisture-Density Relationships	12
Strength Analysis	13
Influence of Calcium Activator	13
Influence of Moisture Content	13
Influence of Compaction Energy	14
Influence of Curing Time	14
HFA Base and Pavement Design	15
Field Construction	15
Field Testing	16
Field Performance	17
Surface Distress Observations	17
Evaluation of Core Strength	17
Durability Investigation	19
Conclusions	20
Acknowledgements	21
References	22
CHAPTER III. MICROSTRUCTURE OF COMPOSITE MATERIAL FROM HIGH-LIME FLY ASH AND RPET	34
Abstract	34
Introduction	35

Material and Methods	36
Material	36
Composite Material Production	38
Test Methods	39
Results and Discussion	40
Effect of Composite Material Loading	40
Stress-Strain Properties	41
Properties of Composite Material	42
Composite Bonding Characteristics	43
DSC Study in Heating and Cooling Mode	43
Summary and Conclusions	45
Acknowledgements	45
References	46
Notation	47
CHAPTER IV. SIMPLIFIED AND RAPID SOIL PERFORMANCE CLASSIFICATION SYSTEM	59
Abstract	59
Introduction	59
Background	62
Soil Identification	62
In Situ Embankment Profiles	63
Development of the EPC System	64
Clayey Soils	65
Silty Soils	67
Empirical Performance Classification (EPC) Chart	68
EPC Procedure	69
Classification Criteria	70
High Plasticity Clays	70
Medium Plasticity Clays	71
Low/Medium Plasticity Clays	71
Low Plasticity Clays	72
Silts of Medium Compressibility	72
Highly Compressible Silts and High Plasticity Organic Clays	73
Conclusions	73
Acknowledgements	74
References	75
CHAPTER V. GENERAL CONCLUSIONS	87
Long Term Strength and Durability of Hydrated Fly Ash Road Bases	87
Microstructure of Composite Material from High-Lime Fly Ash and RPET	88
Empirical Performance Classification for Cohesive Embankment Soils	88
GENERAL ACKNOWLEDGEMENT	90



## LIST OF FIGURES

	Page
CHAPTER II.	
Figure 1. Particle size distribution of reclaimed HFA	26
Figure 2. (a) ASTM C593 strength development and (b) 28-day humid cure strength	27
Figure 3. Strength sensitivity of HFA/activator mixture to (a) compaction moisture content and (b) compaction energy	28
Figure 4. Long-term laboratory strength development of CKD and AFBC activated HFA	29
Figure 5. (a) Observed pavement condition in CKD activated HFA test section at 5 years of service and (b) edge cracking and raveling in a few locations of the AFBC activated HFA test section	30
Figure 6. Long term CKD activated HFA strength from extracted field cores	31
Figure 7. Demonstration project (a) 10% CKD stabilized core sample showing HFA aggregate and cementitious matrix and (b) core hole showing pavement section	32
Figure 8. Freeze-thaw durability of CKD and AFBC activated HFA mixtures	33
CHAPTER III.	
Figure 1. Composite material with high-lime fly ash spheroids embedded in RPET binder.	51
Figure 2. Variation of compressive strength as a function of fly ash content.	52
Figure 3. Polarized reflective light images at 60× indicating variation in RPET crystal content with fly ash content (a) 70% fly ash, (b) 20% fly ash.	53

Figure 4.	Illustration predicting failure mechanisms of composite material (a) fly ash inhibits propagation of crack, and (b) crack propagation around fly ash spheroid at interface through crystalline RPET.	54
Figure 5.	Variation of split-cylinder tensile strength as a function of fly ash content.	55
Figure 6.	Effect of fly ash concentration on the stress/strain response of composite material.	56
Figure 7.	Sheared surface of fly ash plerosphere embedded in composite RPET binder.	57
Figure 8.	Tightly bound interface of composite material at sheared surface of embedded sand grain.	57
Figure 9.	DSC thermograms of remolded RPET and composite material with 44.4% fly ash content.	58

#### CHAPTER IV.

Figure 1.	Swell potential of recently constructed cohesive embankment based on empirical relationship from Weston (1980) $SP = 0.00411(LL_w)^{4.17}q^{-0.386}w_o^{-2.33}$	82
Figure 2.	Swell potential of recently constructed cohesive embankment based on empirical relationship from Weston (1980) $SP = 0.00411(LL_w)^{4.17}q^{-0.386}w_o^{-2.33}$	83
Figure 3.	Relationship between clay content and plasticity index for Iowa soils	84
Figure 4.	Relationship between measured silt content and predicted silt content from empirical data correlation based on plasticity index and fines content for Iowa soils	85
Figure 5.	Empirical Performance Classification (EPC) chart	86

## LIST OF TABLES

	Page
 CHAPTER II.	
Table 1. Chemical constituents and physical properties	24
Table 2. Optimum moisture content for various mixtures of HFA and calcium activator	25
Table 3. Comparative pavement cost estimates for 0.80 km (0.5 mile)	25
Table 4. Core strength data from AFBC activated HFA section	26
 CHAPTER III.	
Table 1. Chemical constituents and physical properties of fly ash	48
Table 2. Physical and mechanical properties of PET resin	49
Table 3. Comparative properties of composite material	50
Table 4. DSC transition temperatures and enthalpy changes of composite material	51
 CHAPTER IV.	
Table 1. Current Iowa DOT specification for cohesive soil classification into "select", "suitable", and "unsuitable" categories	77
Table 2. Relationship between swell potential and soil index properties	78
Table 3. Relationship between frost susceptibility and soil index properties	79
Table 4. Iowa EPC criteria for cohesive soils	80
Table 5. Comparison of Empirical Performance Classification with AASHTO and Unified soil classification systems	81

## **CHAPTER I. GENERAL INTRODUCTION**

### **Dissertation Organization**

This dissertation is a compilation of three papers submitted to or published in scholarly geotechnical engineering and civil engineering materials journals. The first paper describes an evaluation of the long-term performance of roadbase materials constructed from waste by-products including hydrated fly ash (HFA) with cement kiln dust (CKD) and atmospheric fluidized bed combustion (AFBC) residue used as calcium activators. Field construction processes, material cost estimates and comparisons, and strength and volumetric stability data are analyzed. The second paper describes a newly invented composite material from high-lime (ASTM Class C) fly ash and recycled polyethylene terephthalate (PET) plastic. Development of this value added composite material resulted in Iowa State University filing for a U.S. patent in 1999. The third paper presents a newly developed soil classification system for use in construction of cohesive earth embankments for highway construction. The described system is under review by the Iowa Department of Transportation for adoption and inclusion in statewide design and construction specifications.

Each paper includes references to literature reviewed, research data and significant findings and conclusions with suggestions for future research, and acknowledgements identifying the funding agency sponsoring the research. In the following, a general introduction is presented for the purpose of describing the research problem and significance of each paper. Following the main body of the dissertation is a general conclusion that

summarizes significant research findings from each paper and provides additional recommendations for future research.

### **Long Term Strength and Durability of Hydrated Fly Ash Road Bases**

In order to significantly increase fly ash utilization and reduce long-term waste disposal problems, high volume, alternative applications need to be developed. One of the most promising of these applications is the use of reclaimed hydrated fly ash (HFA) as a replacement for aggregate in road bases. Reclaimed HFA in Iowa is produced at sluice pond disposal sites for generating stations burning low sulfur, sub-bituminous coal. The production of HFA is initiated by dumping and dozing raw fly ash into the sluice pond where it hydrates to form a working surface platform. The HFA is then constructed on top of the platform in thin layers of raw ash that are spread, watered, compacted and allowed to hydrate before the next layer is placed. After cementitious and pozzolanic reactions have hardened the HFA, it is typically mined by using conventional recycling-reclaiming equipment to pulverize and reclaim the material where it is stockpiled on-site for use as an artificial aggregate or structural fill material. When re-moistened and compacted for use as a base material, pozzolanic reactions resulting from unreacted calcium, silica and alumina in the glassy phase of the HFA material contribute to strength gain as a function of time.

This research paper presents the laboratory testing results, design, field construction, and long-term (5 years) performance of a field demonstration project where road base materials were constructed from reclaimed HFA with atmospheric fluidized bed combustion (AFBC) and cement kiln dust (CKD) used as calcium activators. The use of AFBC and CKD

as activators is of interest because these materials are also by-products and must otherwise be landfilled as waste. The physical and chemical properties of these materials in their raw and hydrated form were studied. In addition, the compaction characteristics, crushing strength, freeze-thaw susceptibility, and volumetric stability were evaluated. Strength testing and chemical analysis indicate that AFBC and CKD activators increase cementitious and pozzolanic reactions in the HFA material. Field results of long-term strength gain from core samples show significant strength increase in the CKD stabilized HFA base mixture, while the AFBC stabilized HFA mixture shows signs of freeze-thaw durability problems as opposed to satisfactory laboratory performance under ASTM C593 testing, or volumetric stability problems. It appears that the AFBC section is performing well but is probably functioning as a flexible aggregate base rather than a stabilized and cemented semi-rigid base. The strength properties and environmental benefits of using reclaimed HFA make it a desirable road base material from an engineering, environmental, and economical perspective.

### **Microstructure of Composite Material from High-Lime Fly Ash and RPET**

This technology feasibility study was aimed at converting fly ash and polyethylene terephthalate (PET) wastes into a useful value added composite building material. Objectives of this study were to determine the optimum combination and quantities of fly ash and PET based on favorable mechanical properties and to determine the process parameters for the production of the composite material. In the composite material the fly ash acts as the filler material and the PET plastic acts as the binding material. The fly ash, which is a waste

by-product produced in coal-fired power plants, is available in large quantities. Further, PET is not an environmentally biodegradable material that must be land filled as waste. Thus, recycling has emerged as a practical method to deal with the problem of fly ash and PET plastic disposal. However, in order to achieve a higher reclamation level for fly ash and plastics, value added and secondary products must be developed.

In an effort to develop a new value added product, tests on composite material from high-lime (ASTM class C) fly ash and recycled PET were conducted. First, composite test specimens of fly ash and PET were heated, mixed, and molded to investigate the mechanical properties and microstructure features. Microstructural features associated with crack propagation during compression loading and the PET binding mechanisms were studied using scanning electron and polarized reflective light microscopy and differential scanning calorimetry. The results of this investigation showed that the fly ash concentration contributed significantly to both the strength of composite material and the crystallinity of the PET binder. Second, composite specimens with varying fly ash concentrations were tested in compression and tension, immersed in water to measure water absorption, and observed for shrinkage during manufacturing. The composite material is shown to have high compressive strength (4 to 5 times higher than Portland cement concrete), low density, and low water absorption. Furthermore, it can be molded to form various shapes and contains cementitious properties at fractured surfaces from exposed fly ash particles.

Primary uses for this material are anticipated to be construction panels, masonry units and lightweight polymer aggregate for concrete. Plastic recyclers that make alternative products for fencing and masonry and manufacturers who use lightweight aggregates in their products would be interested in this material. Based on the evidence, it is concluded that the

composite material is a value-added material with a variety of potential construction applications.

### **Simplified and Rapid Soil Performance Classification System**

Considering the complex engineering properties of soils and several unique property correlations, the Empirical Performance Classification (EPC) system was developed to improve overall soil design and facilitate field identification during highway embankment construction. This system of classifying cohesive soils for earth embankments is based on determination of the fraction finer than the No. 40 (425- $\mu\text{m}$ ) and No. 200 (75- $\mu\text{m}$ ) sieves, liquid limit, and plasticity index. The EPC system identifies three major soil performance groups: (1) select, (2) suitable, and (3) unsuitable. Select treatment materials are those placed directly under the pavement structure to provide adequate volumetric stability, low frost potential, and adequate bearing capacity. Suitable soils underlay the select treatment materials and are usually susceptible to seasonal changes such as wetting and drying cycles. Unsuitable materials are commonly characterized as highly plastic clays or highly compressible frost prone silt and are usually buried beneath the suitable soils. The unsuitable soils are further characterized for disposal by one of three methods: (1) slope dressing only, (2) 1.0 m below top of subgrade, or (3) 1.5 m below top of subgrade.

Development of the EPC system is based on empirical relationships for swell potential and frost susceptibility derived from the literature. Also, the new AASHTO group index empirical formula is used as a means of averaging the effects of plasticity index, liquid



limits, and percent passing the No. 200 sieve. A description of the critical engineering properties and values used to develop the system are described.

Classification of soils with the EPC system is ultimately intended to increase field soil identification, better link design with construction, and reduce long-term pavement maintenance costs. Recently, this classification method was used in Iowa on a highway pilot project to test feasibility. Research shows that the EPC system is an effective tool to use when soils are being mixed in the borrow excavation or are not identified during the initial site investigation.

## **CHAPTER II. LONG TERM STRENGTH AND DURABILITY OF HYDRATED FLY ASH ROAD BASES**

A paper submitted to the Transportation Research Record

David J. White<sup>1</sup> and Kenneth L. Bergeson<sup>1</sup>

### **ABSTRACT**

This paper presents long-term performance monitoring of a demonstration project where road base materials were constructed from reclaimed hydrated fly ash (HFA) with atmospheric fluidized bed combustion (AFBC) and cement kiln dust (CKD) by-products used as calcium activators. Reclaimed HFA is a form of artificial aggregate produced from compacted, hydrated Class C fly ash at pulverized coal combustion facilities. Strength testing and chemical analysis indicate that AFBC and CKD activators increase cementitious and pozzolanic reactions in the HFA material. Laboratory analysis determined the preferable range of activator to HFA artificial aggregate ratios for AFBC and CKD activated mixtures based on strength development and freeze/thaw durability analysis, as well as compaction characteristics and optimum moisture content ranges. Results of long-term strength gain from core samples show significant strength increase in the CKD stabilized HFA base mixture, while the AFBC stabilized HFA mixture shows signs of freeze-thaw durability problems as opposed to satisfactory laboratory performance under ASTM C593 testing, or volumetric stability problems. It appears that the AFBC section is still performing well but is probably functioning as a flexible Macadam base rather than a stabilized and cemented semi-

---

<sup>1</sup> Pre-Doctoral Research Associate and Professor, respectively, Department of Civil and Construction Engineering, Iowa State University

rigid base. Long term testing indicates that the high-volume alternative use of these by-products is an economical and suitable application when used with a suitable calcium activator.

## **INTRODUCTION**

Over 40 percent of the electricity produced in the United States is from burning approximately 700 million metric tons of coal annually (1). This results in a significant disposal problem of 90 million metric tons of coal combustion by-products of which approximately 58% is fly ash (2). At the present time it is estimated that 25 percent of fly ash is effectively diverted from the waste stream and used as a material resource (2,3). The greatest volumes of fly ash are used in engineering applications such as concrete products, roadbase materials, and structural fills (4). Other uses for fly ash include mine reclamation, waste stabilization and filler in paint, plastic and metal. While these are excellent applications of fly ash utilization, they typically are low volume uses. For example, fly ash as a mineral admixture in Portland cement concrete only replaces from 10 to 20 percent by weight of cement. In order to significantly increase fly ash utilization and reduce disposal problems, higher volume applications need to be developed. One of the most promising of these applications is the use of reclaimed hydrated fly ash (HFA) as a replacement for aggregate in road bases.

Reclaimed HFA in Iowa is produced at sluice pond disposal sites from generating stations burning low sulfur, sub-bituminous coal. Production of HFA is initiated by dumping and dozing raw fly ash into a sluice pond where it hydrates to form a working surface platform. The HFA is then constructed on top of the platform in thin layers of raw

ash that are spread, watered, compacted and allowed to hydrate before the next layer is placed.

The self-cementing property of Class C fly ash occurs from the initial rapid hydration of tricalcium aluminates and other compounds, which form cementitious reaction products, followed by slower pozzolanic reactions. After initial cementitious reactions have hardened the HFA, it is typically mined by using conventional recycling-reclaiming equipment to pulverize and reclaim the material where it is stockpiled on-site. When re-moistened and compacted, long-term pozzolanic reactions resulting from unreacted calcium, silica and alumina in the HFA material result in significant strength gain as a function of time. With the addition of a calcium activator to the reclaimed HFA, strength development can be significantly enhanced.

The objective of this paper is to present the laboratory testing results, design, field construction, and long-term (5 years) performance of a field demonstration project where road base materials were constructed from reclaimed HFA with atmospheric fluidized bed combustion (AFBC) and cement kiln dust (CKD) used as calcium activators. The use of AFBC and CKD as activators is of interest because these materials are also by-products and must otherwise be land filled as waste. The physical and chemical properties of these materials in their raw and hydrated form were studied. In addition, the compaction characteristics, crushing strength, freeze-thaw susceptibility, and volumetric stability were evaluated.

## **MATERIAL PROPERTIES**

### **Reclaimed Hydrated Fly Ash (HFA)**

Reclaimed HFA produced in Iowa is from Class C fly ashes that typically contain 20 to 30 percent crystalline compounds including free calcium oxide and tricalcium aluminates. These crystalline compounds are primarily responsible for the initial rapid hardening and early strength gain of HFA. The remaining 70 to 80 percent of the fly ash is composed of glassy phases (5). The glassy phase, rich in calcium, aluminum and silica, is believed to be a reactive glass (i.e. chemically dissolves more rapidly than silica rich glass) (6). Long term strength gain of reclaimed HFA is believed the result of pozzolanic reactions from the slow dissolution of the calcium, aluminum and silica in the glassy phase, which are still present in the reclaimed HFA after initial hardening.

The reclaimed HFA evaluated in this study was produced at the Ottumwa Generating Station (OGS) in Ottumwa, Iowa. Analytical chemical composition of this material is shown in Table 1. Figure 1 shows the particle size distribution, indicating that the HFA produced was reasonably well graded with about 20 percent fines content (7).

### **Cement Kiln Dust (CKD)**

Cement kiln dust (CKD) is a by-product of Portland cement production. It is generated from the process of removing alkalis, chlorides, and sulfates from cement kiln exhaust gasses and is collected by either a bag house or electrostatic precipitator (8). Typically, CKD is a fine material with a mass median particle diameter of approximately 10  $\mu\text{m}$  (9). The CKD used in this investigation was obtained from the Lafarge cement plant in Buffalo, Iowa. Similar to Class C fly ash, CKD when hydrated will form cementitious

reaction products. In contrast, CKD typically has a much higher affinity for water than fly ash requiring up to 50% water before becoming slurry (9).

### **Atmospheric Fluidized Bed Combustion (AFBC) Residue**

In recent years one of the clean coal technologies that has been developed to meet stricter sulfate emission standards is the production of atmospheric fluidized bed combustion (AFBC) residue. AFBC residue is formed by burning pulverized coal mixed with a limestone sorbent in a fluidized bed at temperatures near 900°C (10). Chemical reactions between the sulfur in the coal and sorbent trap the sulfur while in the combustion chamber, which then becomes part of the solid by-product. Through this process the limestone is reduced to calcium oxide and becomes part of the pozzolanic material in the by-product (11). Consequently, two to four times more solid waste is generated than in standard pulverized coal-fired plants (8).

Table 1 shows the chemical constituents of the CKD and AFBC residue. In comparison to the reclaimed HFA, the CKD contained approximately two times the calcium oxide content and four times the sulfate content. The calcium oxide content of the AFBC is similar to that of the reclaimed HFA but also has four times the sulfate content. It has been reported that the influence of high sulfate content in lime and fly ash stabilized soil can result in high initial strength, but may compromise durability by affecting the normal long-term pozzolanic reactions of the stabilizing process (12,13). Furthermore, the potential for development of expansive minerals such as ettringite and thaumasite increases (13,14).

## **LABORATORY TESTING**

The following presents the results of materials testing and initial design of the reclaimed HFA base for the Ottumwa-Midland landfill access road. The landfill access road is 0.8 km long and supports local traffic and heavily loaded trucks transporting power plant by-products to the landfill disposal site. Moisture-density relationships, strength development and freeze-thaw durability (predicated from ASTM C593) were the primary criteria used in the design.

### **Moisture-Density Relationships**

Moisture-density tests were conducted using standard Proctor energy and ASTM D 698 test procedures. The moisture-density curves for the HFA with both CKD and ABFC activators are relatively flat (i.e. little change in density with increasing water content). Optimum moisture content was selected for each mixture based on the moisture-density data and compactibility of the mixes. Results are shown in Table 2. On average, optimum moisture content and maximum dry density for untreated HFA materials from Iowa are in the range of 26-36 percent at 12.4-14.6 kN/m<sup>3</sup> (79-93 lb/ft<sup>3</sup>) maximum dry density (15). Specific gravity of the raw fly ash is about 2.7, while the HFA bulk specific gravity and the saturated surface dry (SSD) bulk specific gravity are typically 1.5 and 1.9, respectively. During the reclaiming process, it was observed that in-situ moisture content of the reclaimed HFA varied from 14 percent near the surface to 24 percent at 0.5 m. If enough water is available reclaimed HFA will quickly ( $\leq 15$  minutes) absorb water to equilibrate at about 25 to 30 percent moisture.

## **Strength Analysis**

### *Influence of Calcium Activator*

Several crushing strength samples consisting of CKD and AFBC activated HFA mixtures were prepared in standard Proctor molds at approximate optimum moisture content using standard compaction energy. Samples were then humid cured at 38°C (100°F) for 7 days as per ASTM C593 requirements (16). For comparison, three sets of samples were tested under soaked and vacuum saturated test conditions for each treatment level.

According to Dempsey and Thompson (17) vacuum saturation can be used as a rapid and accurate method for predicting freeze thaw durability of materials such as soil-cement, lime-fly ash, and lime soil mixtures. Figure 2(a) shows results of strength testing for 10, 15, and 20 percent CKD and AFBC activated HFA mixtures. ASTM C593 guidelines suggest a minimum strength of 2.8 MPa (400 lb/in<sup>2</sup>) for field performance and freeze-thaw durability of nonplastic mixtures. Untreated the HFA achieved strengths of only 0.3 MPa (50 lb/in<sup>2</sup>) (13). The CKD activated HFA exhibited strengths of about 6.9 MPa (1000 lb/in<sup>2</sup>) at the 10 and 15 percent addition levels; whereas, the AFBC activated HFA exhibited strengths of about 5.5 MPa (800 lb/in<sup>2</sup>) at the 15 and 20 percent levels. For comparison, samples were also prepared and tested as per ASTM C593 procedures except they were cured for 28-days in 100 percent humidity conditions at 21°C (70°F) and are shown in Figure 2(b).

### *Influence of Moisture Content*

To evaluate crushing strength development relative to compaction moisture content, samples were prepared using 15 percent CKD and AFBC activator levels and compacted both dry and wet of optimum moisture content. Test results, shown in Figure 3(a), indicate



that a significant strength reduction occurs for both CKD and AFBC activators when compaction moisture content is below optimum.

#### *Influence of Compaction Energy*

To evaluate effects of compaction energy on strength and density, CKD samples were prepared on the dry and wet side of optimum using compaction energies ranging from 80 percent standard Proctor to modified Proctor energy. AFBC samples were prepared at optimum moisture content using variable compaction energy only. Strength results are shown in Figure 3(b). At 15 percent CKD, samples prepared on the dry side of optimum exhibited dry densities of  $13.5 \text{ kN/m}^3$  ( $86 \text{ lb/ft}^3$ ) at 80 percent standard Proctor energy. At modified energy, density increased to  $14.6 \text{ kN/m}^3$  ( $93 \text{ lb/ft}^3$ ). The CKD samples prepared wet of optimum exhibited dry densities of about  $13.4 \text{ kN/m}^3$  ( $85 \text{ lb/ft}^3$ ) at 80 percent standard and  $14.3 \text{ kN/m}^3$  ( $91 \text{ lb/ft}^3$ ) at modified energy. The crushing strength of the CKD activated HFA slightly increased as compaction energy increased. All AFBC samples exhibited dry densities of about  $13.5$  to  $13.8 \text{ kN/m}^3$  ( $86$  to  $88 \text{ lb/ft}^3$ ) at all compaction energy levels and exhibited similar strengths regardless of compaction energy.

#### *Influence of Curing Time*

AFBC and CKD activated reclaimed HFA mixtures were tested early in the research program for curing periods of up to one year under sealed and humid curing conditions. Results are shown in Figure 4. These tests verify that long-term strength gain takes place and that there is little difference between sealed versus humid cured conditions. It can be seen that the CKD mixture is approximately twice as strong as the AFBC activated HFA.

Through 336 days it is evident that strength curves for both the CKD and AFBC mixtures are trending upwards, thus indicating long-term pozzolanic activity is continuing.

In summary, the laboratory data indicate that (1) CKD and AFBC calcium activators significantly increase initial strength development of the reclaimed HFA and show no signs of freeze-thaw durability problems from ASTM C593 testing, (2) field compaction should be conducted at or above optimum moisture, (3) additional compaction energy does little to increase density or strength, and (4) pozzolanic activity is evidenced by continued long term strength gain.

### **HFA BASE AND PAVEMENT DESIGN**

Based on the laboratory analysis, the pavement section for the test road was designed to consist of 3.8 cm (1.5 inch) asphalt concrete surface course, a 28 cm (11 inch) stabilized reclaimed HFA base at 10 percent CKD or 15 percent AFBC activator levels and a 10 cm (4 in) aggregate subbase for drainage. In addition, an asphalt cement prime coat was specified to act as a curing membrane and bonding agent over the HFA base. Comparative cost estimates of Portland cement concrete and asphaltic cement concrete pavement sections, which were calculated to provide equivalent structural capacity, are shown in Table 3. With an activated HFA base and thin asphaltic concrete surface, it was estimated that the pavement cost could be reduced by 45 to 50%.

### **FIELD CONSTRUCTION**

The Ottumwa-Midland landfill access road was constructed from May 30 through June 1, 1995. In order to compare the performance of both CKD and AFBC as calcium

activators. test sections consisting of a 550 m (1800 ft) section of 10 percent CKD activator and a 210 m (700 ft) section of 15 percent AFBC activator were constructed.

The major steps involved with preparing the CKD and AFBC activated HFA mixtures were as follows:

- HFA reclaimed at OGS sluice pond disposal site
- Activator belly dumped onto a predetermined area of hydrated HFA. spread by motor grader. mixed and reclaimed to depth of about 20 cm (8 in) with CAT RR250.
- Material stockpiled at site

Construction of the base was accomplished in one lift using the following equipment

- CAT tractor and Jersey box spreader
- Seeman's self-propelled pulvimixer
- Two water trucks
- Fifty-ton Buffalo Springfield static pad foot roller for initial deep compaction
- Pneumatic roller for surface compaction
- Vibratory steel wheeled roller for finish compaction
- Motor grader

### **Field Testing**

Quality control moisture-density testing indicated that 95% compaction was achieved in the CKD treated section with moisture averaging 3 percent above optimum. whereas the AFBC section was compacted to 92% compaction at 7 percent above optimum.

Furthermore, several density tests indicated a 5 to 6 percent density variation between the surface and bottom of the base, with the bottom exhibiting lower density. Additional field compaction effort resulted in no increase in density.

## **FIELD PERFORMANCE**

Since construction of the Ottumwa-Midland landfill access road, field performance evaluations have been conducted annually for a period of 5 years. Monitoring includes pavement distress observations and mapping and core sampling for strength determination.

### **Surface Distress Observations**

Both test sections have exhibited transverse and longitudinal thermal cracking of the surface course. These cracks appeared the first summer after construction and have remained tight on both sections over the 5 years observed. The only other pavement distress observed, as shown for the CKD section in Figure 5(a), is some edge cracking and slight raveling of the thin asphaltic concrete surface. This is more pronounced in the AFBC section where the surface course was on the order of 25 mm (1 in) thick as shown in Figure 5(b). This is believed to be due, primarily, to lack of edge and shoulder support of the HFA base. No other evidence of distress has been observed and both test roads are performing well for the intended use under heavy traffic.

### **Evaluation of Core Strength**

Nominal 10.2 cm (4 inch) diameter cores extracted in August 1995 (2 months after construction) show compressive strength averaging 5.7 MPa (830 lb/in<sup>2</sup>) for the CKD

section, and 4.1 MPa (590 lb/in<sup>2</sup>) for the AFBC section. On average a 30 percent strength difference was noted in cores extracted from the CKD section from top to bottom of the base layer with the top being stronger. Annual coring has shown an increase in the strength of the CKD activated base. The range in core strength and combined average results of the top and bottom cores, shown in Figure 6, indicate significant strength increase in the first 2 years up to 15.4 MPa (2230 lb/in<sup>2</sup>). Strength appears to be slightly decreasing over the last 3 years. Figure 7 shows the HFA aggregate and orientation from a core slice of the CKD activated HFA and a core section extracted in June 2000.

In contrast to the CKD test section, the AFBC activated HFA has not shown long-term strength gain. Table 4 summarizes limited core strength data from the first 2 years after construction. Cores extracted the first year were above the 2.8 MPa (400 lb/in<sup>2</sup>) requirement suggested by ASTM C593 for freeze-thaw durability, which agreed with previous laboratory test results. However, the fact that only 1 out of 6 cores were recovered over the next 2 years suggested that HFA base deterioration was occurring. Recent observation of material removed from a 150 mm core hole indicates that the AFBC activated HFA is severely delaminating parallel to the pavement surface in thin angular shaped lenses (50 to 100 mm in rough diameter by 5 to 10 mm thick). The delamination appears to be occurring through the cemented matrix and not through the HFA aggregate particles. It was not known if this is a freeze-thaw durability problem (not evidenced by the ASTM C593 test method) or a volumetric stability problem due to delayed expansive, reaction product formation.

## DURABILITY INVESTIGATION

Following field observations of delamination occurring in the AFBC section, laboratory testing was conducted to evaluate volumetric stability and freeze-thaw durability. First, long-term volumetric stability was analyzed in the laboratory by measuring volume change in test specimens cured at room temperature in different moisture conditions. Three samples of each mixture (10% CKD and 15% AFBC) were cured at room temperature in air, 100% relative humidity, and submerged in water. Results indicated that very little volume change occurred in the AFBC or CKD stabilized HFA (less than 0.5% through 1 year). Again if significant expansive reactions were occurring it was not evidenced over the 1-year testing period under the described curing environments.

A rigorous freeze-thaw test was then developed to evaluate durability and to check the validity of ASTM C593 tests for predicting the freeze-thaw durability of CKD and AFBC activated HFA. Seven samples of AFBC and CKD activated reclaimed HFA mixtures were prepared at optimum moisture content. Samples were then cured in 100 percent humidity for seven days. After the curing period the samples were unwrapped, weighed, resealed in plastic bags and placed in a freezer at  $-17.8^{\circ}\text{C}$  ( $0^{\circ}\text{F}$ ) for three days. After the three-day freezing period, the samples were removed from the freezer and submerged in a water bath at room temperature for four days to thaw. At the end of the four-day thawing period the samples were weighed and placed back into the freezer for another cycle. Results of mass loss per freeze-thaw cycle are shown in Figure 8. It can be seen that the 10% CKD activated reclaimed HFA survived 59 freeze-thaw cycles losing on average 18 percent mass. In sharp contrast, the 15% AFBC samples survived only 9 cycles losing 50 % mass. This finding

suggests that ASTM C 593 is not adequate for predicting freeze-thaw durability of these materials.

Important components of durability analysis for stabilized materials that possess long-term pozzolanic activity (in the presence of sulfates) are curing time and environment (available water for hydration, water quality, temperature). It is known that the primary cementitious reaction product present in HFA is ettringite (15). If sulfates are available to the cementitious matrix in the proper temperature environment, ettringite can transform to thaumasite, which is a highly hydrous and expansive mineral (14). However, thaumasite only forms from ettringite at temperatures below 15°C. Therefore, it is speculated that ettringite may have first formed in the AFBC activated HFA and slowly converted to thaumasite during winter freeze thaw cycles. Thus, initial volumetric studies conducted at room temperature (24°C) did not provide a favorable temperature environment for the conversion. Nevertheless, it cannot be stated with certainty whether or not delamination observed in the AFBC test section was initiated by freeze-thaw action or expansive reaction product formation. Additional experiments involving x-ray and thermal analysis are underway to better understand the long-term durability of CKD and AFBC activated HFA and untreated HFA.

## **CONCLUSIONS**

The principal conclusions of the laboratory and long-term field performance study described in this paper are as follows:

- The use of HFA appears to be an economical and suitable alternative to conventional road base materials. Pavement material costs can be significantly reduced by 45 to 50 percent.
- By-products containing high levels of sulfates may not be appropriate as a calcium activator for long-term durability.
- HFA material is unique in that if water is available for hydration long-term pozzolanic reactions increase strength with time. Unlike conventional granular base materials. Long-term strength gain was evidenced in the laboratory and from extracted core samples.
- ASTM C593 freeze-thaw durability testing does not appear to be applicable to AFBC and CKD activated HFA because long term pozzolanic activity and potentially expansive reaction product formation is not a variable in the test method.
- Despite the delamination occurring in the AFBC activated HFA test section, it has been performing very well under heavy traffic loads through 5 years. The only pavement distress observed is some edge cracking and raveling of the thin asphaltic concrete surface on both the CKD and AFBC activated HFA test sections, which is believed to be due to inadequate edge and shoulder support.

## **ACKNOWLEDGEMENTS**

The authors would like to thank the Iowa Fly Ash Affiliate Research Program and participating utilities for sponsoring this project.



**REFERENCES**

1. Bakkar. W.T. Production of Properties of Fly Ash. *Utilization of Ash Workshop*. University of North Dakota. Grand Forks. North Dakota. May 13-15. 1987.
2. *American Coal Ash Association*. Coal Ash - Innovative Applications of Coal Combustion Products (CCPs). Alexandria. Virginia. 1998.
3. Tarricone. P. Fly Ash for Hire. *Civil Engineering*, October 1991. pp. 46-49.
4. U.S. Department of Transportation. Fly Ash Facts for Highway Engineers. *Rep. No. FHWA-SA-94-081*, Federal Highway Administration. Washington. D.C.. 1995.
5. Bergeson. K.L. The Glassy Phase and Reaction Products of Iowa Fly Ashes. Ph.D. Dissertation. Iowa State University. 1986.
6. Diamond. Sidney. On the Glass Present in Low-Calcium and High Calcium Fly Ashes. *Cement and Concrete Research*. Vol. 13. 1983. pp. 459-464.
7. IES Utilities Ottumwa-Midland Landfill Access Road. Pavement Bases from Waste by-Products. Field Demonstration Project Report. *ERI Project 3009*. Iowa State University. Ames, April 1996.
8. Bergeson. K.L. Iowa Fly Ash Affiliates Research Program. Annual Report. *ISU-ERI-Ames 96-410*. Iowa State University. Ames, December 1995.
9. Portland Cement Association. An Analysis of Selected Trace Metals in Cement and Kiln Dust. *SP109T*. Skokie. Illinois, 1992.
10. Rangaraju, P., and C.L. Kilgour. Hydration Reactions of FBC By-Products From Iowa Power Plants and Their Use In Concretes. EPRI TR-104656-V1. Proceedings:

*Eleventh International Symposium on Use and management of Coal Combustion By-Products*. Vol. 1, Orlando, Florida, January, 1995.

11. *American Coal Ash Association International*. Soil and Pavement Base Stabilization with Self-Cementing Coal Fly Ash. Alexandria, Virginia, May 1999.
12. Ferguson, Glen. Use of Self-Cementing Flay Ashes as a soil Stabilization Agent. *Presented at the ASCE National Meeting*, Dallas, Texas, 1993.
13. Kota, P.B.V.S. , Hazlett, D., and Perrin, L. Sulfate-Bearing Soil: Problems with Calcium-Based Stabilizers. *Transportation Research Record* 1546. TRB, National Research Council, Washington, D.C. 1997, pp.62-69.
14. Hunter, D. Lime-Induced Heave in Sulfate-Bearing Clay Soils. *ASCE Journal of Geotechnical Engineering*, Vol. 114, No. 2, 1988, pp.150-167.
15. Bergeson, K.L. Iowa Fly Ash Affiliates Research Program. Annual Report. *ISU-ERI-Ames 98-401*, Iowa State University, Ames, December 1997.
16. American Society for Testing and Materials. Annual Book of ASTM Standards. Section 4. Construction. Vol. 4.01. Philadelphia, Pennsylvania, 1994.
17. Dempsey, B.J. and Thompson, M.R. Vacuum Saturation Method for Predicting Freeze-Thaw Durability of Stabilized Materials. *Highway Research Board 442*. TRB, National Research Council, Washington, D.C. 1973, pp.44-57.
18. Bergeson, K.L. Iowa Fly Ash Affiliates Research Program. Annual Report. *ISU-ERI Ames 99501*, Iowa State University, Ames, December 1998.

**TABLE 1 Chemical constituents and physical properties**

Chemical Composition	Base Materials (mass %)		
	HFA	CKD	AFBC
Silicon dioxide (SiO <sub>2</sub> )	31.0	15.5	23.8
Aluminum oxide (Al <sub>2</sub> O <sub>3</sub> )	16.9	3.8	9.7
Ferric oxide (Fe <sub>2</sub> O <sub>3</sub> )	5.6	1.9	7.0
Sulfur trioxide (SO <sub>3</sub> )	3.6	14.4	15.7
Calcium oxide (CaO)	25.9	52.3	28.4
Magnesium oxide (MgO)	5.7	3.3	8.5
Phosphorous pentoxide (P <sub>2</sub> O <sub>5</sub> )	1.0	0.1	0.3
Potassium oxide (K <sub>2</sub> O)	0.3	4.4	1.0
Sodium oxide (Na <sub>2</sub> O)	3.2	0.6	0.6
Titanium oxide (TiO <sub>2</sub> )	1.3	0.2	0.6
Strontium oxide (SrO)	0.40	0.04	0.06
Barium oxide (BaO)	0.74	<0.02	0.09
LOI (Loss on Ignition) 950°C	4.59	1.71%	6.03
<b>Physical Properties</b>			
Specific Gravity	—	2.88	2.78
Fineness (> #325 sieve. %)	—	37.6	45.7
pH	—	12.57	12.65

**TABLE 2 Optimum moisture content for various mixtures of HFA and calcium activator**

Activator	Activator Content	Optimum Moisture Content (%)	Maximum Dry Density kN/m <sup>3</sup>
CKD	10	27	14.14
	15	27	14.29
	20	28	14.45
AFBC	10	27	14.29
	15	28	14.29
	20	29	14.29

**TABLE 3 Comparative pavement cost estimates for 0.80 km (0.5 mile)**

Pavement Section <sup>a</sup>	Estimated Cost
191 mm (7.5 in) PCC pavement (C-4 Iowa DOT concrete mixture)	\$145,000
Full-depth ACC pavement consisting of 216 mm (8.5 in) of black base and 51 mm (2 in) of surface course	\$143,000
Activated HFA base 279 mm (11 in) thick with 38 mm (1.5 in) hot-mix asphalt cap	\$76,000

<sup>a</sup> All pavement section estimated to provide equivalent structural numbers

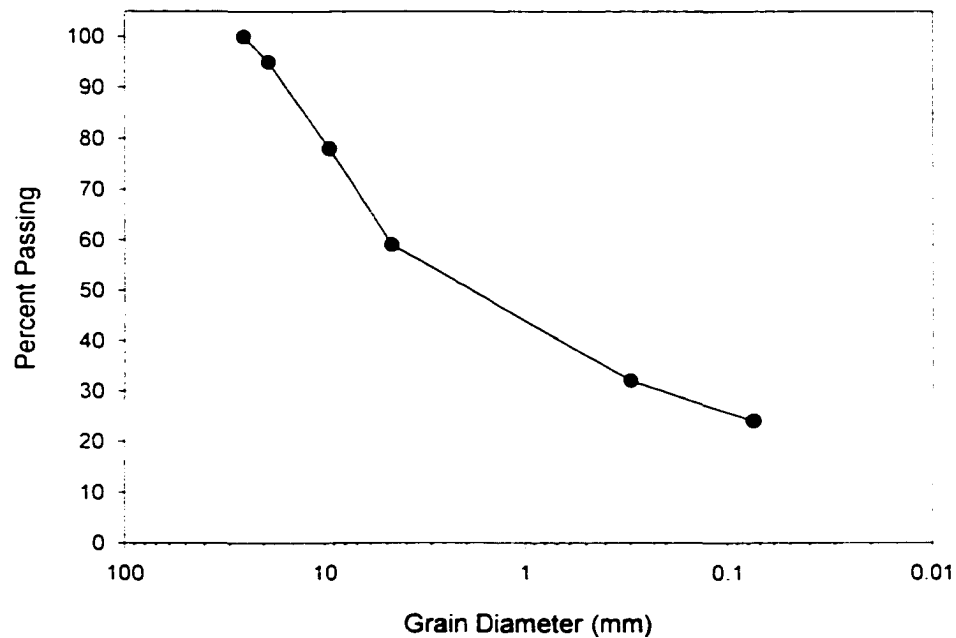
**TABLE 4 Core strength data from AFBC activated HFA section**

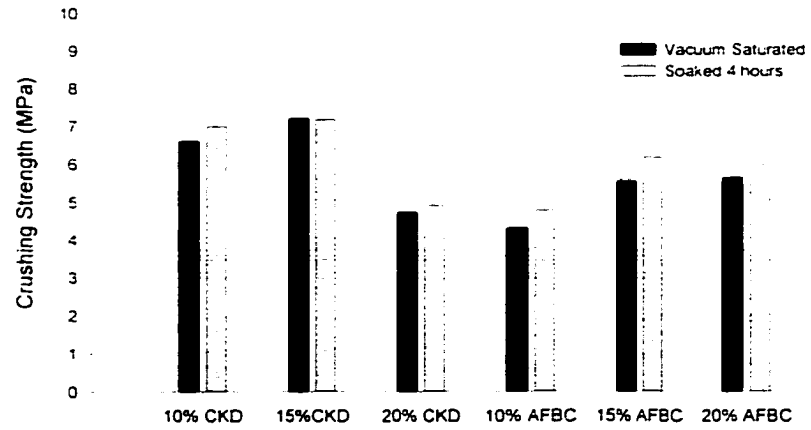
Sample <sup>c</sup>	Strength Range MPa	Standard Deviation MPa	Number of Samples	Average Strength MPa (lb/in <sup>2</sup> )
August 1995	2.21-6.41	1.9	5 <sup>a</sup>	4.1
May 1996	—	—	1 <sup>b</sup>	8.96

<sup>a</sup> Out of 4 core samples only one had sufficient recovery to get a top and bottom test

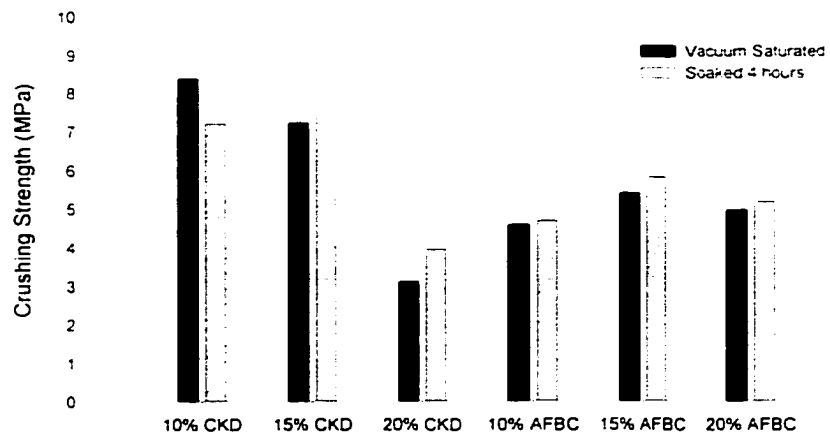
<sup>b</sup> Four cores were attempted only 1 could be extracted

<sup>c</sup> In 1997 two cores were attempted with no recovery

**FIGURE 1 Particle size distribution of reclaimed HFA**



(a)



(b)

**FIGURE 2 (a) ASTM C593 strength development (b) 28-day humid cured strength**

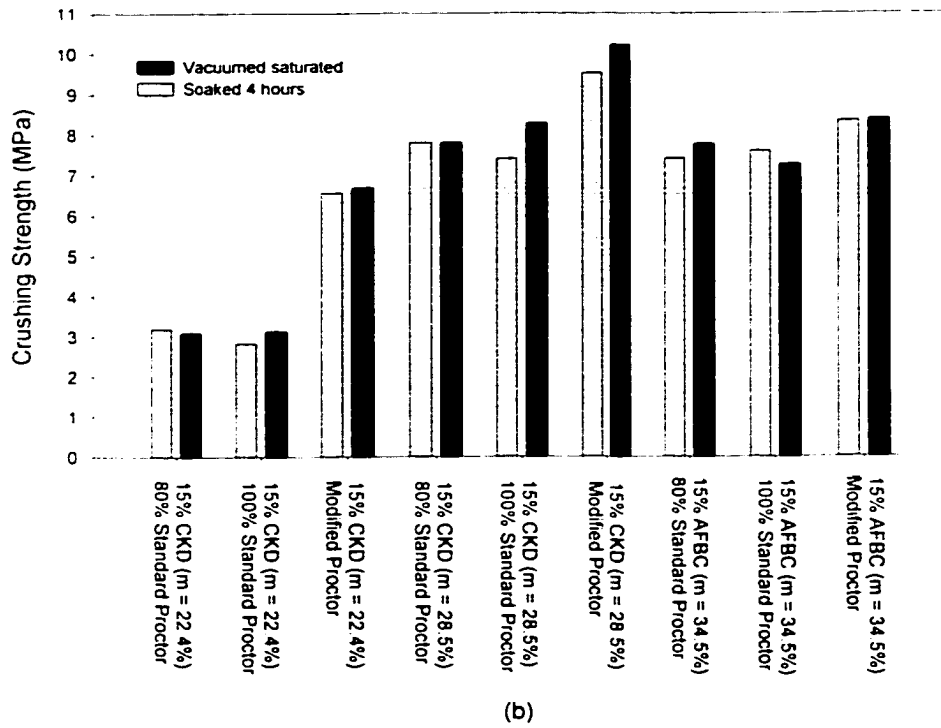
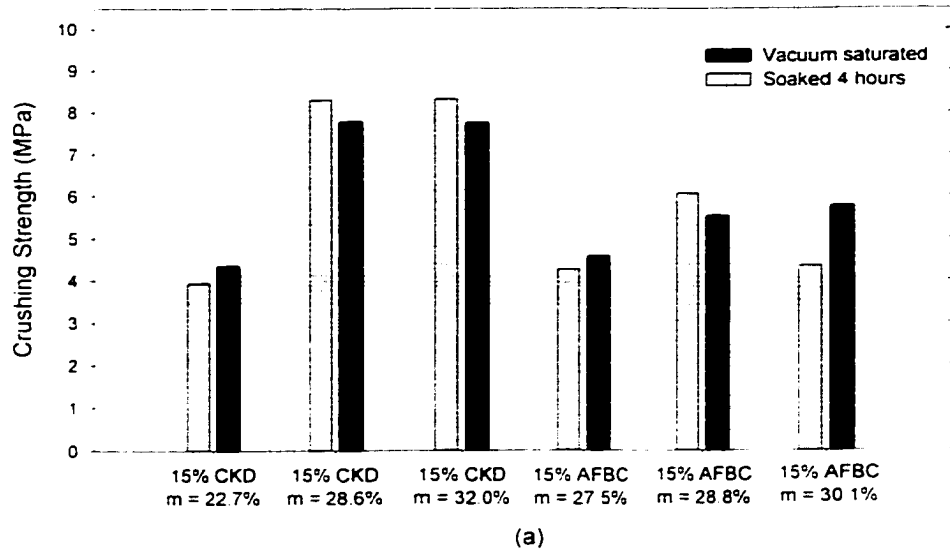


**FIGURE 3 Strength sensitivity of HFA/activator mixture to (a) compaction moisture content and (b) compaction energy**

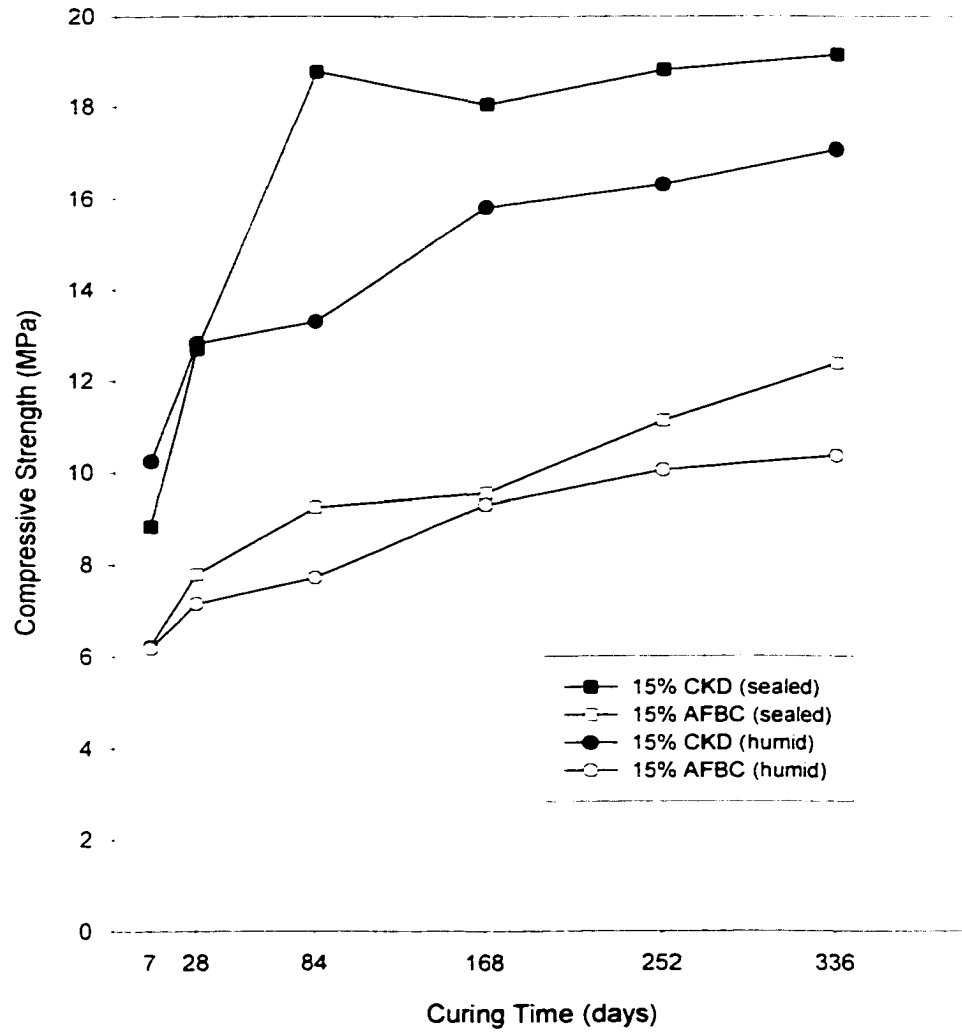
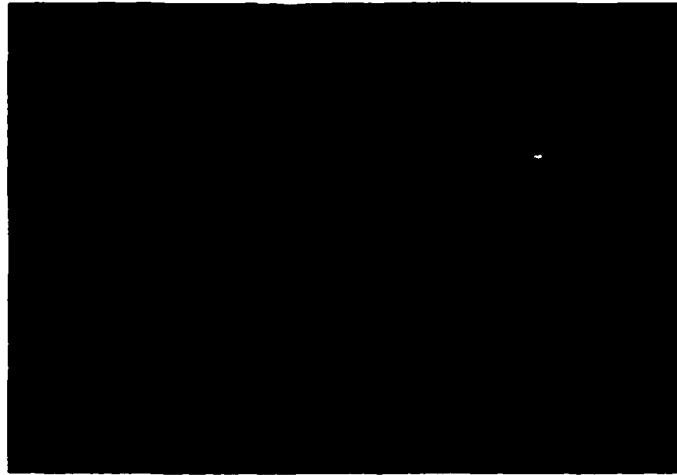
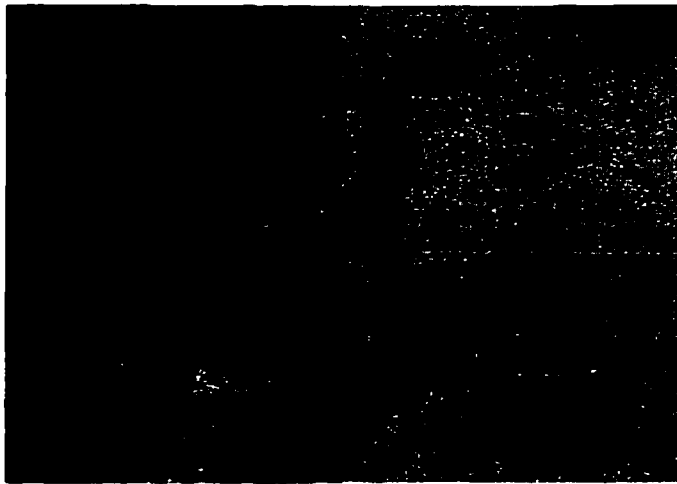


**FIGURE 4 Long-term laboratory strength development of CKD and AFBC activated HFA**





(a)



(b)

**FIGURE 5 (a) Observed pavement condition in CKD activated HFA test section at 5 years of service and (b) edge cracking and raveling in a few locations of the AFBC activated HFA test section**

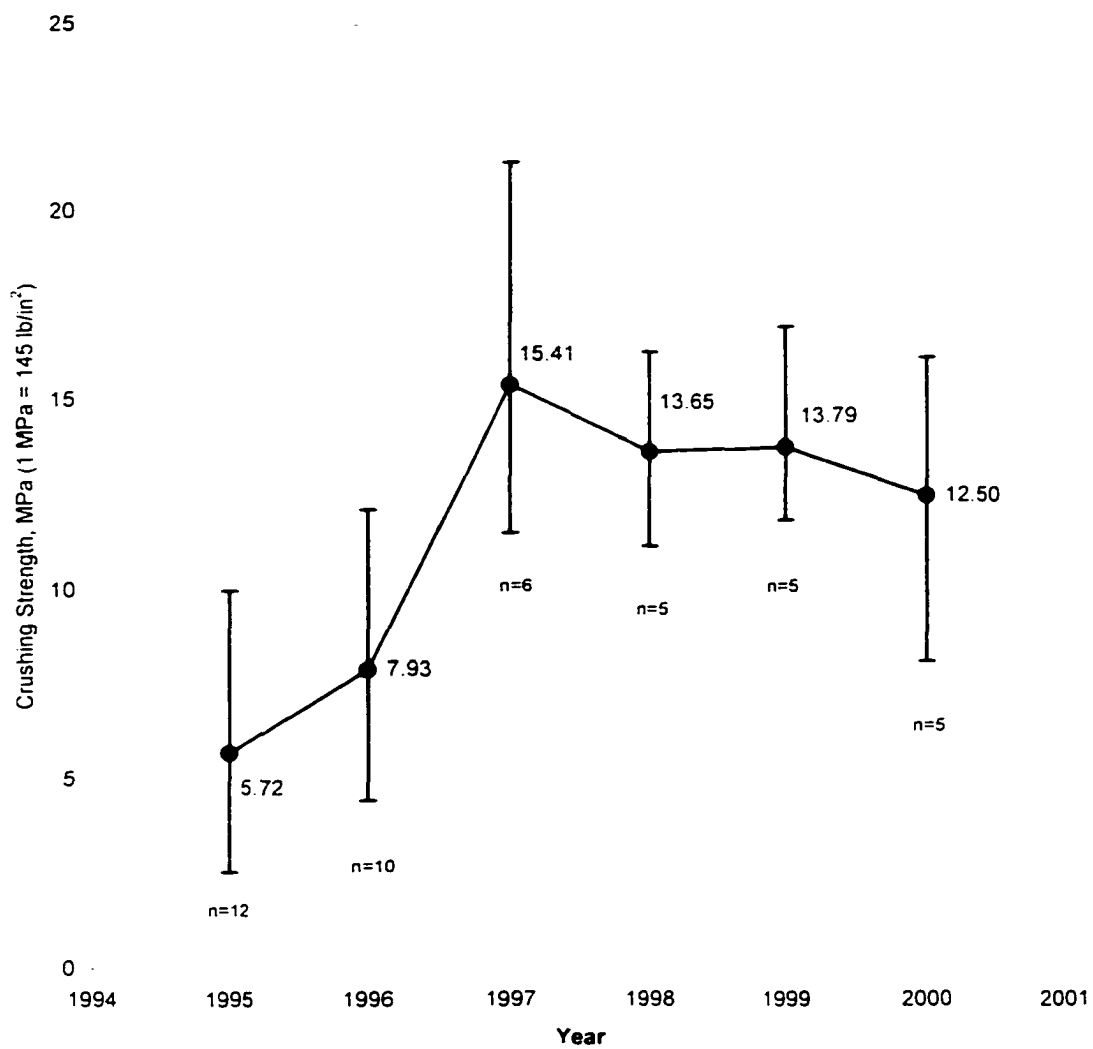
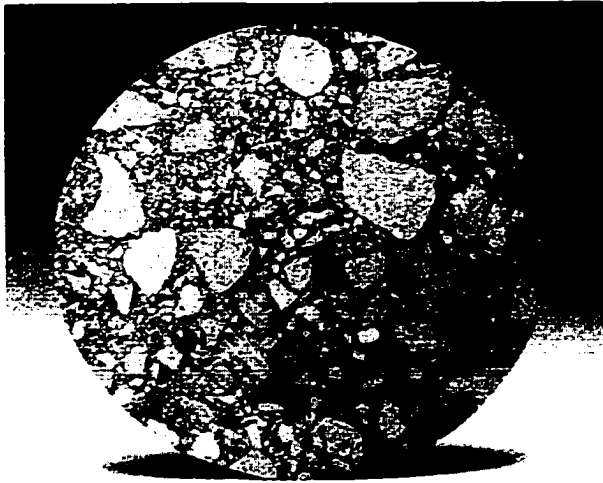


**FIGURE 6 Long term CKD activated HFA strength from extracted field cores**



(a)



(b)

**FIGURE 7 Demonstration project (a) 10% CKD stabilized core sample showing HFA aggregate and cementitious matrix (b) core hole showing pavement section**

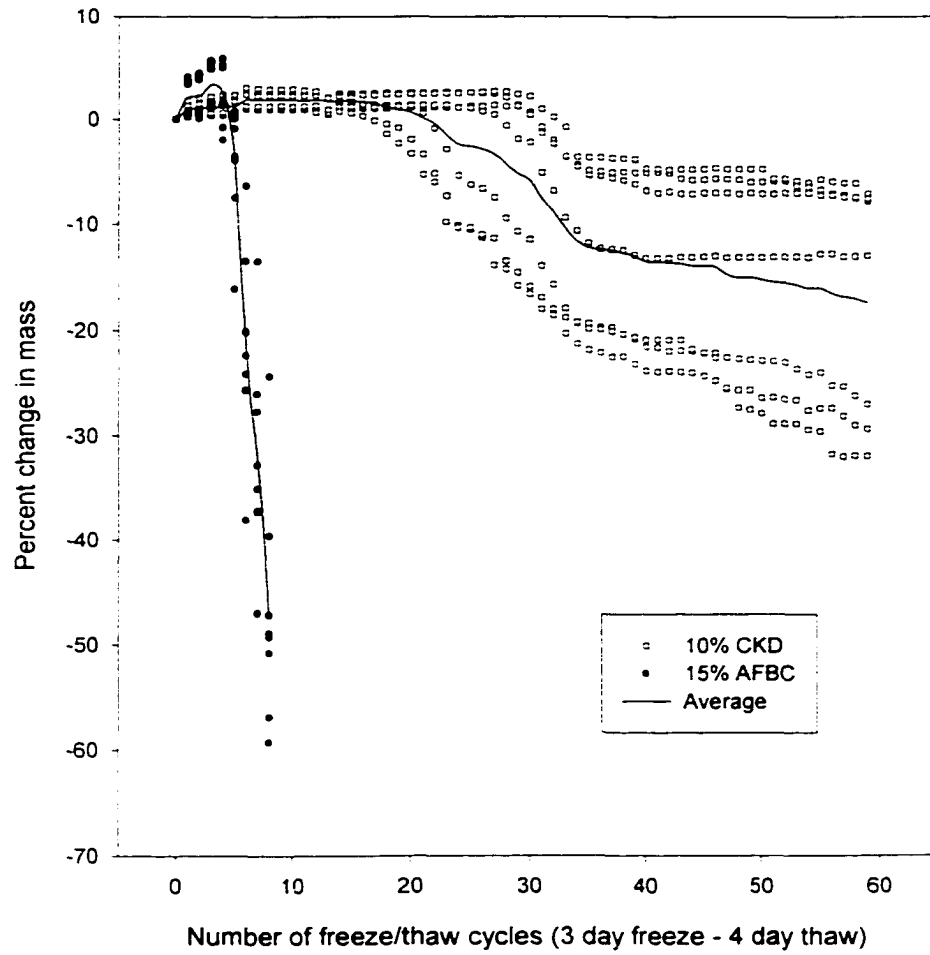


**FIGURE 8 Freeze-thaw durability of CKD and AFBC activated HFA mixtures**

### **CHAPTER III. MICROSTRUCTURE OF COMPOSITE MATERIAL FROM HIGH-LIME FLY ASH AND RPET**

A paper published in the *Journal of Materials in Civil Engineering*<sup>1</sup>

David J. White<sup>2</sup>

#### ABSTRACT

Tests on composite material from high-lime (ASTM class C) fly ash and recycled polyethylene terephthalate (RPET) were conducted to investigate the physio-mechanical properties and microstructure features. Composite specimens with varying fly ash concentrations were tested in compression and tension, immersed in water to measure water absorption, and observed for shrinkage during manufacturing. Theoretical equations from modulus of elasticity and tensile strength were derived with values compared to Portland cement concrete. Microstructural features associated with crack propagation during compression loading and the RPET binding mechanism were studied utilizing scanning electron and polarized reflective light microscopy and differential scanning calorimetry. The results of this investigation showed that the fly ash concentration contributed significantly to both the strength of composite material and the crystallinity of the RPET binder. Based on the evidence, it was concluded that the composite material is a value-added material with a variety of potential construction applications.

---

<sup>1</sup> Reprinted with permission of *Journal of Materials in Civil Engineering*, 2000, 12(1), 60-65

<sup>2</sup> Pre-Doctoral Research Associate, Department of Civil and Construction Engineering, Iowa State University

## INTRODUCTION

Recognizing the environmental benefits, the production and use of waste materials such as fly ash and plastics has been strongly favored by environmental agencies. With this incentive an alternative composite material from high-lime cementitious fly ash and recycled post-consumer polyethylene terephthalate (RPET) has been developed.

High-lime fly ash, selected as filler, is a by-product of coal combustion in electric-generating stations that burn subbituminous coal. Millions of tons of fly ash are generated in the United States each year. Currently, the greatest volumes of cementitious fly ash are used in engineering applications such as concrete products, roadbase materials, and structural fill materials (U.S. Dept. of Trans. 1995). The remaining unused fly ash is usually pumped to sluice ponds or transported to landfills as waste, constituting long-term waste management problems.

Waste PET plastic is neither environmentally biodegradable nor compostable, which creates disposal problems. Recycling has emerged as the most practical method to deal with this problem, especially with products such as PET beverage bottles, where the recycling process is fairly straightforward. Currently, a large waste stream is available for recycling applications. In the U.S., estimates indicate that production of PET containers will reach  $1.8 \times 10^6$  kg by the year 2000, which is a 55% increase from 1997 (Gabriele 1997). Along with increases in waste production, the incentive to develop recycling technologies and value added materials is amplified. In order to achieve a higher reclamation level for plastics, such as RPET, various secondary products must be developed (Chen and Shiah 1989). In terms of the processes of melting, mixing and homogenizing, recycled RPET from beverage bottles

has been found to be a favorable type of plastic to mix with high-lime fly ash and was selected as the binder component for the composite material.

The objective of this paper is to improve the understanding of some mechanical properties and the strength gain mechanism of the composite material. Effects from compressive and tensile loading were evaluated along with density and water absorption. Polarized reflective light microscopy and differential scanning calorimetry (DSC) were utilized to analyze the PET crystalline content with variations in fly ash concentration. Scanning electron microscopy (SEM) was utilized to develop an understanding of the microstructure bonding and shear mechanism.

## **MATERIALS AND METHODS**

### **Materials**

Fly ash is produced in electric-generating stations by burning finely ground coal at about 1500°C. The type of fly ash produced, typically characterized as high-lime or low-lime, depends on the type of coal burned (Cohen 1995). For the composite material a high-lime (ASTM class C) fly ash was chosen as the filler material and was produced from combustion of low-sulfur, subbituminous coal that originated from the Powder River Basin near Gillette, Wyoming (Bergeson et al 1988). Low carbon, high calcium content and self-cementitious properties characterize this fly ash. The chemical analyses from x-ray fluorescence are given in Table 1 along with fineness and specific gravity.

Typically, high-lime (ASTM class C) Iowa fly ash contains from 20 to 30 percent analytical lime. Physically, they contain more fine and less coarse particles than low-lime (ASTM class F) fly ash (Cohen 1995). Chemically, they usually are composed of 20 to 30

percent crystalline compounds with the remainder being amorphous, glassy materials. The fly ash spheroid particles and particle size distribution are shown embedded in the composite material in Figure 1. After sampling the fly ash, the moisture content of the fly ash was maintained at less than 1%, reducing hydration and pozzolanic reactions prior to composite production.

RPET, which is a thermoplastic polymer, can consist of either a completely amorphous structure or a partially crystalline structure. The crystalline portion of the RPET forms because thermoplastics have completely separated molecules that can crystallize by rearrangement and ordering of the molecules (Miller 1996). Similar to all crystalline solids, this creates an internal repeating order of molecules or atoms. Upon heating, RPET and other thermoplastics polymers can melt, becoming sufficiently free flowing to permit mold filling (Miller 1996). In addition, these crystalline polymers have a sharp, identifiable melting point (MacDermott and Shenoy 1997). In the production of the composite material both amorphous and partially crystalline RPET containers were utilized. By observation the physical difference between the amorphous and crystalline RPET can be seen, since amorphous RPET is typically transparent and crystalline RPET is opaque.

Transparent, opaque and green post-consumer RPET beverage bottles were utilized in the production of the composite material, which were acquired through a local collection effort. In order to prepare and process the RPET, the plastic was first rinsed in warm water to remove any residue. Next, the bottle caps, labels and adhesives were physically removed. Once washed and air-dried, the bottles were shredded to nominal square sizes of 0.5 to 6.0 cm. This simple laboratory recycling and processing operation emulates commercial RPET recycling processes that typically consist of the following steps: (1) segregation of the



bottles. (2) air separation to remove metal and paper. (3) flotation to remove non-RPET flakes. and (4) final drying (Basta et al. 1997). Table 2 contains details of some typical mechanical properties of PET resin used in the production of beverage bottles. Virgin PET resin used in the production of beverage bottles has a crystallinity that is normally about 25% (Ehrig 1992).

### **Composite Material Production**

In order to manufacture the composite material and perform engineering property testing, proportions of dry fly ash and shredded RPET were heated, homogenized, and molded to form testing specimens. Heating was accomplished by placing the fly ash and shredded RPET in an open container over an electric burner. During heating the temperature was controlled between 255 and 265°C to induce melting of the RPET but not to exceed the decomposition temperature (approximately 270°C). While being heated the crystalline property of the RPET brought about an obvious transition temperature from solid to liquid. The composite material was homogenized by stirring the mixture. The smooth spherical shape of the glassy fly ash spheroids significantly contributed to the homogenization of the mixture.

Since the mechanical properties of the polymer composite depend more strongly on the manufacturing process than those of other materials (Miller 1996), the influence of molding temperatures and cooling rates on the composite material were monitored. Once heated and homogenized, the mixtures were poured into a variety of preheated molds to form the specified geometry for testing purposes. Next, the composite material and molds cooled

synchronously at room temperature for approximately 2 hours. For testing purposes, some samples were cut or machined to form flat parallel ends.

Fly ash concentration in the composite specimens ranged from 0 to 70 percent by dry weight of the total mixture. Fly ash concentrations over 50% significantly increased the mixing time to obtain a homogeneous mixture, and mixtures over 70% were not possible with the described production methods. Upon cooling, the composite material had a hard, smooth texture, light brown color and was non-transparent. When crystallization occurs, it has been found that transmission of light through polymers is known to decrease (Fann et al 1998).

## **TEST METHODS**

Fly ash sampling and classification was conducted in accordance with ASTM C 311 and ASTM C 618. Specific gravity was measured utilizing a helium pycnometer. Compressive strength of the composite material was determined according to ASTM D 695 at a loading rate of 5 mm/min. Split-cylinder tensile strength was performed as per ASTM C 496-86 at a loading rate of 5 mm/min. A material testing system (MTS) was used to test stress-strain characteristics. Deformation readings were taken at a loading rate of 5 mm/min. Microstructural features were studied utilizing a Hitachi model S-2460N scanning electron microscope and an Olympus BHM polarized reflective light microscope with a Pixera Color CCD color system. Differential scanning calorimetry tests were performed with a model 2960 TA Instrument DSC. The samples were heated at a rate of 15 °C/min in the temperature range of 50 to 325 °C. Immersing the samples into boiling water for 2 hours and measuring the change in mass was used to evaluate water absorption.

## **RESULTS AND DISCUSSION**

### **Effect of Composite Material Loading**

Cylindrical test specimens with a diameter of 26 mm and a height of 52 mm were manufactured for evaluation of compressive and tensile strength. The compressive strength results are shown on Figure 2. Compressive strength increased from approximately 77 to 111 MPa with increasing fly ash contents from 0 to 65 percent, respectively. The strength gain may be attributed to the increasing crystallinity in the RPET portion of the composite material as the fly ash content increases. During molding the fly ash is believed to act as a thermal insulator. This reduces the cooling rate and increases the crystallinity of the RPET by allowing the RPET molecules to arrange themselves in an ordered pattern. As shown on Figure 3, images from a polarized reflective light microscope show that the crystallinity increases (indicated by bright colored grains) with increasing fly ash content. During compressive loading the fly ash particles and crystallinity of the RPET at interfaces inhibit crack propagation. In addition, solid, glassy fly ash spheroids increase the shear stress area between the interface of fly ash particles and the RPET binder. Figure 1 shows the fractured surface of the composite material and is evidence of strong bonding between the fly ash and RPET. For comparison, the illustration in Figure 4 depicts the hypothesized variation of RPET crystalline boundaries due to the fly ash and a predicted model of crack propagation.

Due to the lack of complete fly ash particle coverage, beyond approximately 65 to 70 percent fly ash content, the compressive strength decreased as shown on Figure 2. At high fly ash concentrations interfacial bonding could possibly be enhanced with increased mixing and homogenization. Results indicate that at 65% fly ash content the compressive strength is 4 to 5 times higher than ordinary portland cement concrete. As previously reported by Li et

al. (1998), a composite material from post-consumer RPET and low-lime (ASTM class F) fly ash possessed compressive strengths 3 to 4 times that of ordinary portland cement concrete.

The strength of the composite material in tension is an important property that greatly affects the extent and size of cracking at failure (Wang and Salmon 1992). Results of tensile strength tests are shown on Figure 5. Tensile strength varied from 3 to 7 MPa for fly ash contents of 0 to 70 percent with 50% being about optimum. The split-cylinder tensile strength  $f_{ct}$  has been found to be proportional to the compressive strength  $f'_c$  such that:

$$f_{ct} = 0.4 \text{ to } 0.7\sqrt{f'_c} \quad (1)$$

where  $f_{ct}$  and  $f'_c$  are in units of MPa.

Over a fly ash concentration of about 50%, the tensile strength decreased, conceivably due to an increased area of fracture planes. Despite its plastic nature the composite tensile strength was highly variable and was about 4 to 6 percent of the compressive strength, which is comparable to concrete (Wang and Salmon 1992).

### **Stress-Strain Properties**

Compressive strength stress-strain curves for composite specimens made with fly ash concentrations of 0, 37.5 and 70 percent are shown on Figure 6. From this data, it was observed that at 0% fly ash content, the remolded RPET was relatively ductile. Upon increasing the fly ash concentration, the stiffness increased and the composite material became more brittle. Therefore, given the same stress levels, increased fly ash content decreases the strain at failure. Elastic modulus values of the composite material ranged from

1185.7 MPa at 0% fly ash to 2252.3 MPa at 70% fly ash, which are on the order of 10 times less than that of ordinary Portland cement concrete. Such a finding is important if the composite material is considered for use in areas of energy and impact attenuation (Delwar et al 1997). For fly ash concentrations  $C_{FA}$  between 0 and 60 percent the elastic modulus of the composite,  $E_c$ , data collected suggests:

$$E_c = 125 \text{ to } 135 \left(1 + \frac{C_{FA}}{100}\right) \sqrt{f'_c} \quad (2)$$

where  $E_c$  and  $f'_c$  are expressed in units of MPa and  $C_{FA}$  expressed as percent dry weight of the total mixture.

### **Properties of Composite Material**

Values of average strength, elastic modulus, density, water absorption, and shrinkage are shown in Table 3. The density of the composite material varies from 1.28 to 2.03 g/cm<sup>3</sup> for fly ash content of 0 to 70 percent. Thermodynamic shrinkage during manufacturing decreased from 2.2% with no fly ash to 0.7% with a 70% fly ash concentration. Water absorption was very low and variable from 0 to 0.9 percent. The fly ash particles, as shown on Figure 1, are actually coated with a thin layer of tightly bonded RPET preventing exposure to water. However, at fractured surfaces, sheared cenosphere and plerosphere fly ash particles and some solid, glassy fly ash spheroids were exposed and susceptible to water exposure. With this in mind the cementitious properties of the high lime-fly ash particles in the composite material could be taken advantage of by expanding the potential uses of the material. For example, if the composite material was utilized in-place of conventional

masonry brick where it would be exposed to mortar, the bond between the mortar and fly ash particles in the composite material could increase the overall strength of the masonry system. Overall, the low density and high-lime fly ash makes it an alternative for a variety of construction materials such as light to medium weight concrete aggregate or lightweight construction panels.

### **Composite Bonding Characteristics**

As previously reported it was observed that a composite material with ASTM class F fly ash and RPET could not be completely homogenized (Li et al 1998). However, as shown on Figure 1, it appears as though the high-lime (ASTM class C) fly ash particles are completely homogenized and coated with RPET. Figure 7 indicates a tightly bound plerosphere sheared in half along a fractured surface. To further investigate the ability of the composite material to physically bond and adhere to materials, ordinary concrete sand was mixed with the composite material. Figure 8, shows the tightly bound interface between a sand grain and the composite material along a fractured surface. The bonding strength of the composite material has been shown to exceed the shear strength of cenosphere and plerosphere fly ash particles, solid, glassy fly ash spheroids and common concrete sand grains.

### **DSC Study in Heating and Cooling Mode**

To further study the crystalline behavior of the composite material and to provide insight into the effects of fly ash concentration on RPET crystallinity, DSC studies in the heating (endothermic) and cooling (exothermic) mode were performed. A sample of

remolded RPET with no fly ash and a 44.4% fly ash sample were cut from the surfaces of fractured specimens. The average sample weight was 7.2 mg. The thermograms are shown on Figure 9 and were used to calculate the peak melting temperature  $T_m$ , peak cooling crystallization temperature  $T_c$ , and the corresponding enthalpy changes  $\Delta H$ . The results are displayed in Table 4. Note below approximately 1500°C the fly ash particles are inert and do not melt within the DSC test temperature range.

The  $T_m$ 's for remolded RPET with no fly ash and a composite mixture with 44.4% fly ash were 246.7°C and 250.4°C, respectively. The difference of 3.7°C is on account of the variations in crystallinity induced in the RPET by fly ash. As the crystalline structure becomes more ordered,  $T_m$  will increase (Fann et al. 1998). The remolded RPET with no fly ash consists of a lower amorphous fraction than the 44.4% composite mixture of RPET and fly ash. Therefore, due to its crystalline component and more orderly molecular structure (Fann et al. 1998), the  $T_m$  of the composite material with increased fly ash content is higher than that of the composite material at low fly ash concentrations.

The RPET exotherm associated with crystallization shifts to a lower temperature with increasing cooling rates (Fann et al. 1998). Peak cooling crystallization temperatures for the remolded RPET with no fly ash and 44.4% fly ash in the composite mixture were 205.4°C and 215.9°C, respectively. Thus, a relationship exists between the fly ash concentration in the composite material and the RPET peak cooling temperature of crystallization. The fly ash in the composite material manifests an increase in  $T_c$  by reducing the cooling rate during manufacturing. With this in mind the influences of fly ash and cooling rates during manufacturing could have a significant impact on material properties. According to Bergenn

et al. (1985). some advantages of higher crystallinity include greater resistance to organic solvents and dynamic fatigue.

## **SUMMARY AND CONCLUSIONS**

The results of this research have shown that a value added composite material has been developed from high-lime (ASTM class C) fly ash and recycled RPET. In addition to environmental incentives for utilization of waste materials, favorable mechanical properties such as low density, minimal water absorption and high compressive strength create several potential uses for the composite material. The cementitious properties of the high-lime fly ash at fractured surfaces add diversity to potential products and applications for the composite material such as masonry brick and concrete aggregate.

It has been shown that fly ash plays a critical role in cooling rates and crystallinity of the RPET binder, which allows for an influence of mechanical properties through manufacturing. The crystallinity of RPET is an important mechanism that is directly related to the fracture mechanics of the composite material. Further, high-lime fly ash has been found to be economical as filler in the composite material reducing potential manufacturing costs.

## **ACKNOWLEDGEMENTS**

The writer would like to thank the John H. Faber Scholarship Program administered by the American Coal Ash Association (ACAA) for providing the opportunity to research this topic. Special thanks are due to Dr. Kenneth L. Bergeson and Dr. Scott Schlorholtz for helpful discussions, suggestions, and valuable advice and for assistance through the Material



Analysis and Research Laboratory (MARL) at Iowa State University. Also, thanks are due to the Iowa Fly Ash Affiliates for materials and laboratory support.

## REFERENCES

- Basta, N., Ondrey, G., Rajagopal, R., and Kamiya, T., (1997). "Plastics recyclers scramble for scraps." *Chemical Engineering* 104(6), 43-119.
- Bergenn, W., and Rigby, R. B., (1985). "Tough engineering thermoplastics." *Chemical Engineering Prog.*, Jan. 36-38.
- Bergeson, K. L., Schlorholtz, C., Demirel, T., (1988). "Development of a rational characterization method for Iowa fly ash." *Iowa DOT Project HR-286, Engineering Research Institute Project 1847*. Iowa State University, Ames, Iowa.
- Chen, I., and Shiah, C., (1989). "Producing tough PET/HDPE blends from recycled beverage bottles." *Plastics Engineering*, 33-35.
- Cohen, M. D., (1995). "Special cements and concretes." In: Chen, W. F. (Editor-in-chief). *The Civil Engineering Handbook*. CRC Press, New York, N.Y.
- Delwar, M., Fahmy, M., and Taha, R., (1997). "Use of reclaimed asphalt pavements as an aggregate in Portland cement." *ACI Materials Journal* 94(3), 251-256.
- Ehrig, R., (1992). *Plastic recycling*. Oxford University Press, New York, N.Y.
- Fann, M., Huang, S. K., and Lee, J., (1998). "DSC studies on the crystallization characteristics of poly(ethylene terephthalate) for blow molding applications." *Polymer Engineering and Science* 38(2), 265-273.
- Gabriele, M. C., (1997). "PET finds growing use in non-food containers." *Modern Plastics*, 60-65.

- Li, Y., White, D. J., and Peyton, L., (1998). "Composite material from fly ash and post-consumer PET." *Resources, Conservation and Recycling*, 24(2), 87-96.
- MacDermott, C. P., and Shenoy, A. V., (1997). *Selecting Thermoplastics for Engineering Applications*. Marcel Dekker, Inc., New York, N.Y.
- Miller, E., (1996). *Introduction to Plastics and Composites*. Marcel Dekker, Inc., New York, N.Y.
- U.S. Department of Transportation (1995). "Fly ash facts for highway engineers." *Rep. No. FHWA-SA-94-081*, Federal Highway Administration, Washington, D.C.
- Wang, C., Salmon, C. G., (1992). *Reinforced concrete design*. Harper Collins Publishers, New York.

## NOTATION

The following symbols are used in this paper.

- $C_{FA}$  = percent concentration of dry fly ash by total mass
- $E_c$  = modulus of elasticity of composite material
- $f_c$  = compressive strength of composite material
- $f_{ct}$  = split-cylinder tensile strength
- $T_c$  = peak cooling crystallization temperature
- $T_m$  = peak melting temperature
- $\Delta H$  = change in enthalpy

**Table 1. Chemical constituents and physical properties of fly ash**

NO. (1)	Properties (2)	Value (3)
A	Chemical composition	Weight percentage
1	Silicon dioxide (SiO <sub>2</sub> )	30.0
2	Aluminum oxide (Al <sub>2</sub> O <sub>3</sub> )	17.0
3	Ferric oxide (Fe <sub>2</sub> O <sub>3</sub> )	6.4
4	Sulfur trioxide (SO <sub>3</sub> )	4.5
5	Calcium oxide (CaO)	30.2
6	Magnesium oxide (MgO)	7.3
7	Phosphorous pentoxide (P <sub>2</sub> O <sub>5</sub> )	0.9
8	Potassium oxide (K <sub>2</sub> O)	0.3
9	Sodium oxide (Na <sub>2</sub> O)	1.5
10	Titanium oxide (TiO <sub>2</sub> )	1.3
11	Strontium oxide (SrO)	0.4
12	Barium oxide (BaO)	0.8
13	LOI (Loss On Ignition)	0.5
B	Physical properties	
1	Specific gravity	2.68
2	Fineness <sup>a</sup> ( $\geq 10\mu$ )	11.5 %

Note: <sup>a</sup> Data from Bergeson et al (1988). Values are averages based on four years of sampling.

**Table 2. Physical and mechanical properties of PET resin**

No. (1)	Properties (2)	Value (3)	Test Method (4)
1	Tensile Strength	154 (MPa)	ASTM D-638
2	Flexural Strength	231 (MPa)	ASTM D-790
3	Creep Modulus	6895 (MPa)	ASTM D-638
4	Elongation at Break	3 (%)	---
5	Specific Gravity	1.56	ASTM D-792
6	Melting point	254 (°C)	---
7	Average shrinkage	4 – 6 (%)	ASTM D-955

Note: Data from MacDermott and Shenoy (1997) for virgin polyethylene terephthalate resin with 30% crystallinity.

**Table 3. Comparative properties of composite material**

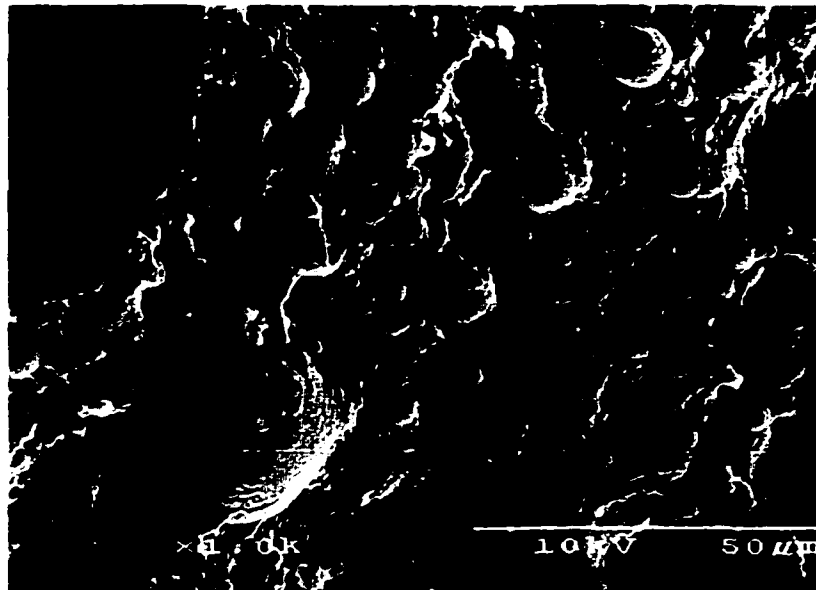
No.	Fly ash content (weight percentage)	Density (g/cm <sup>3</sup> )	Average Experimental Results <sup>(1)</sup>		Modulus of elasticity (MPa)	Water absorption 2 hr (% by wt)	Shrinkage (%)
			Compressive strength (MPa)	Split-cylinder tensile (MPa)			
1	0	1.28	77.4	3.6	1185.7	0.0	2.24
2	9.1	1.32	80.7	3.7	1229.9	0.9	2.02
3	16.7	1.38	81.3	4.0	(2)	0.6	1.88
4	23.1	1.43	90.8	5.1	(2)	0.3	1.85
5	28.6	1.48	90.9	3.9	(2)	0.3	1.80
6	33.3	1.52	90.4	4.3	(2)	0.8	1.47
7	37.5	1.57	89.1	5.0	1572.0	0.7	1.42
8	41.2	1.61	101.3	7.1	(2)	0.5	1.44
9	44.4	1.65	103.0	6.3	(2)	0.8	1.54
10	50.0	1.72	101.7	6.2	2018.4	0.1	1.35
11	54.6	1.79	107.2	6.6	(2)	0.4	1.54
12	60.0	1.87	106.7	4.5	2248.8	0.5	1.25
13	64.3	1.93	111.2	5.5	(2)	0.5	1.33
14	68.8	2.01	100.5	(2)	(2)	0.2	0.96
15	70.0	2.03	(2)	5.6	2252.3	0.2	0.67

(1) Based on two or three samples

(2) Sample was not tested

**Table 4. DSC transition temperatures and enthalpy changes of composite material**

No. (1)	Fly Ash content (%) (2)	$T_M$ (°C) (3)	$T_C$ (°C) (4)	$\Delta H_{melting}$ (J/g) (5)	$\Delta H_{cooling}$ (J/g) (6)
1	0	246.7	205.4	35.7	38.3
2	44.4	250.4	215.9	27.4	28.8

**Figure 1. Composite material with high-lime fly ash spheroids embedded in RPET binder.**

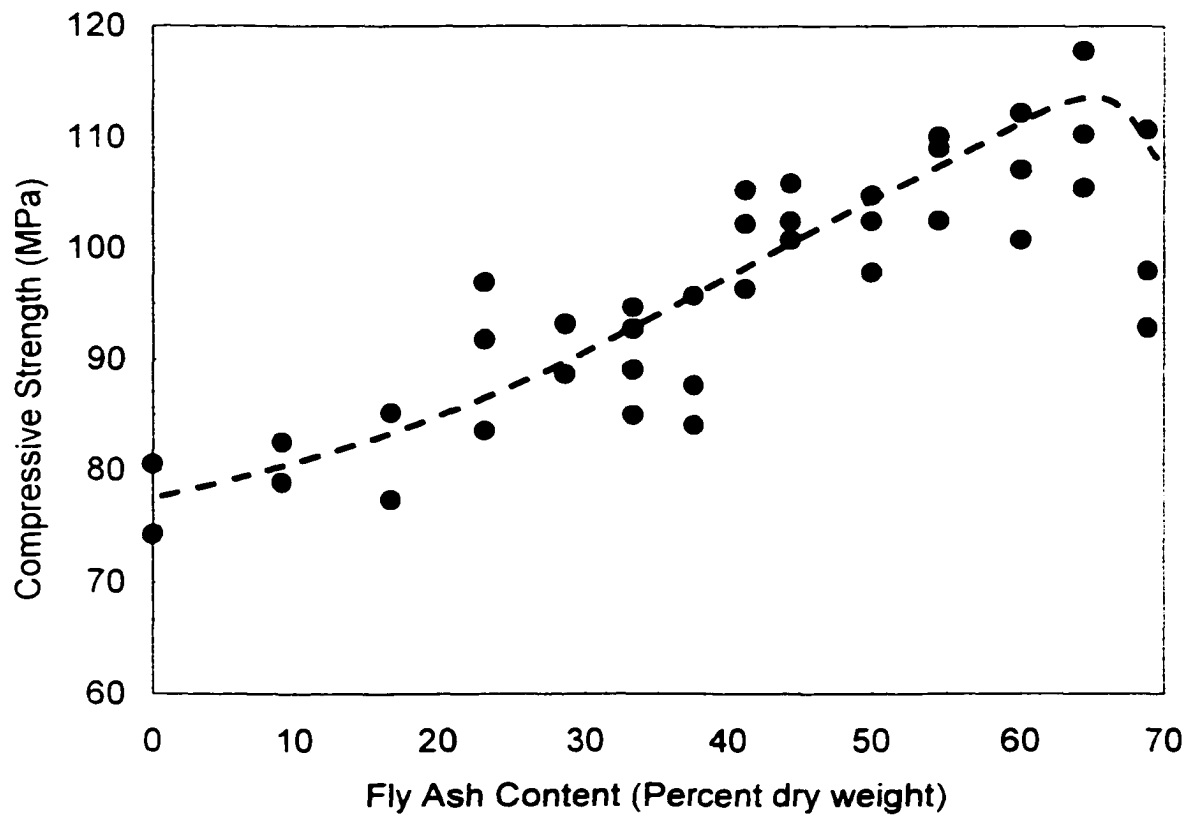
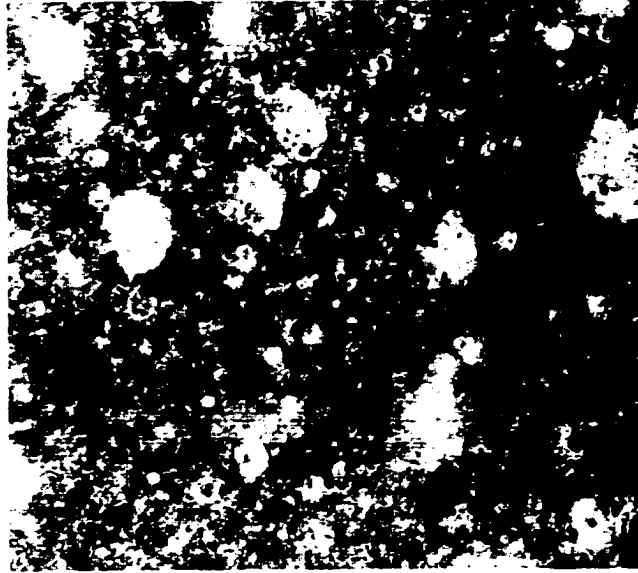
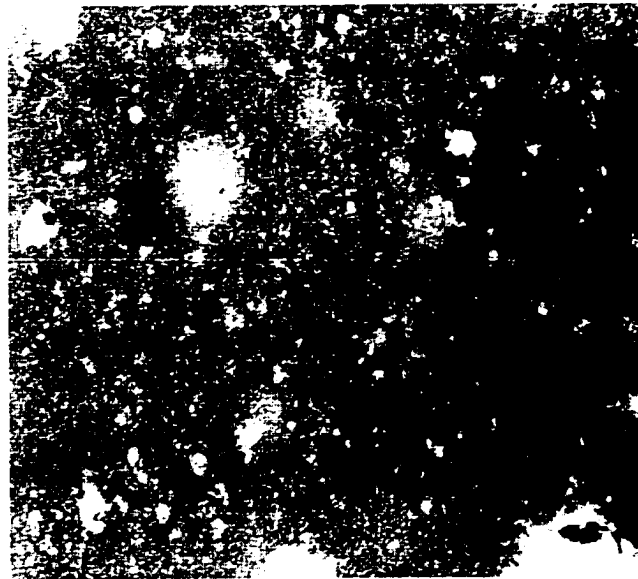


**Figure 2. Variation of compressive strength as a function of fly ash content.**



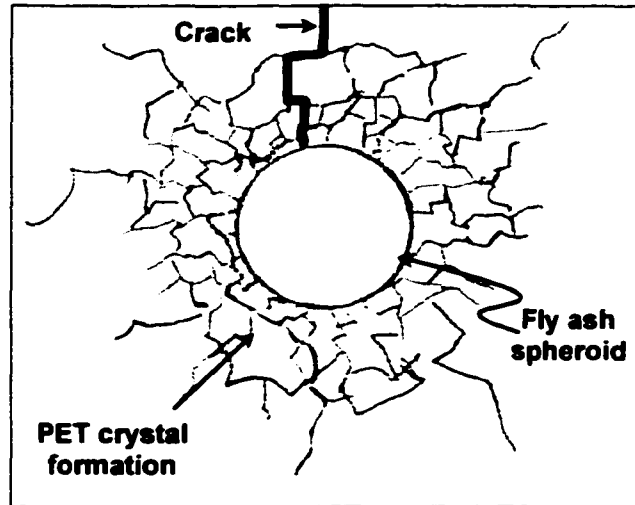
(a)



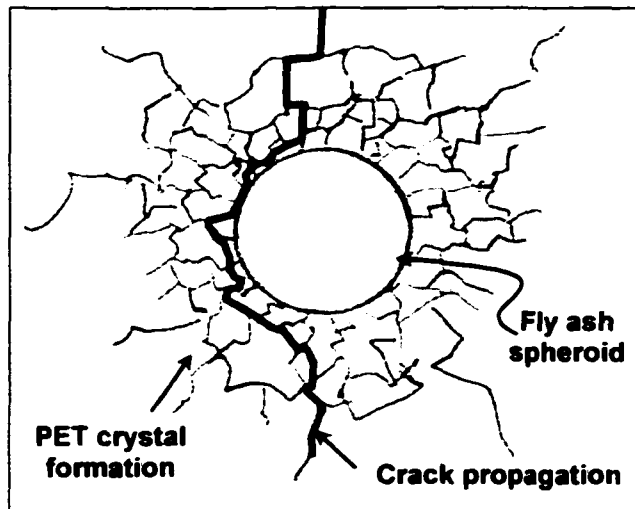
(b)

**Figure 3. Polarized reflective light images at 60 $\times$  indicating variation in RPET crystal content with fly ash content (a) 70% fly ash, (b) 20% fly ash.**





(a)



(b)

**Figure 4. Illustration predicting failure mechanisms of composite material (a) fly ash inhibits propagation of crack, and (b) crack propagation around fly ash spheroid at interface through crystalline RPET.**

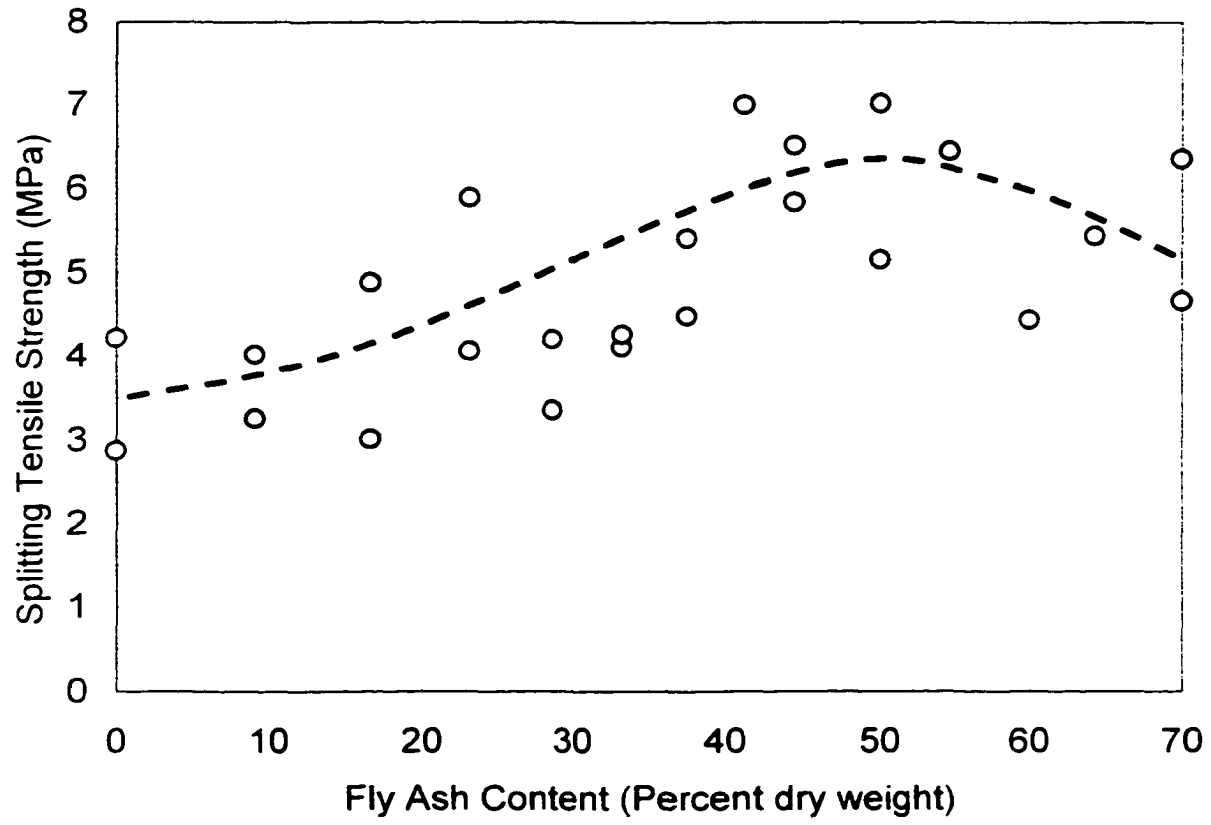


**Figure 5. Variation of split-cylinder tensile strength as a function of fly ash content.**

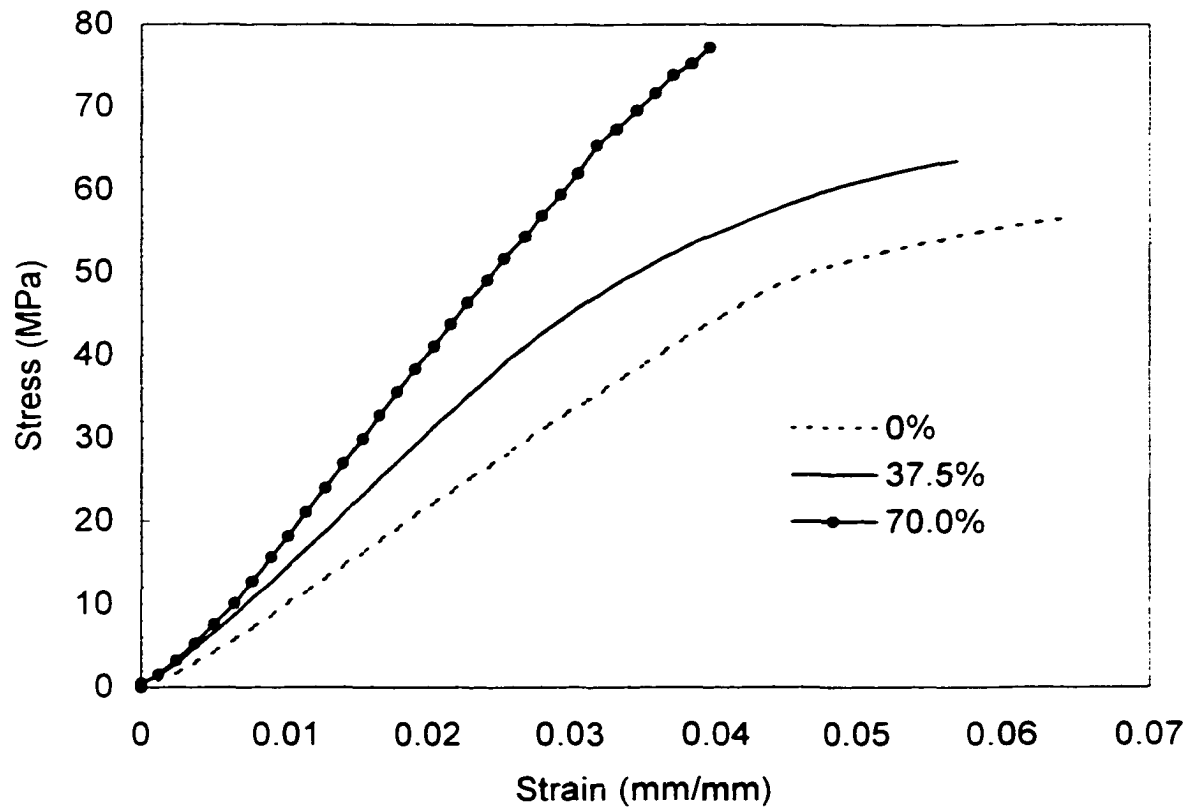


**Figure 6. Effect of fly ash concentration on the stress/strain response of composite material.**

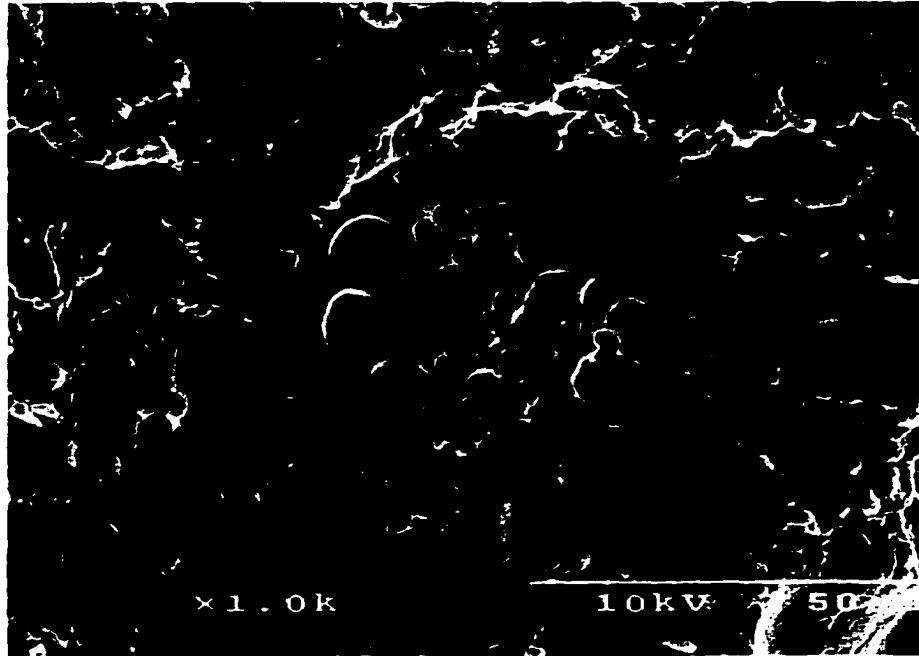


**Figure 7. Sheared surface of fly ash plerosphere embedded in composite RPET binder.**



**Figure 8. Tightly bound interface of composite material at sheared surface of embedded sand grain.**

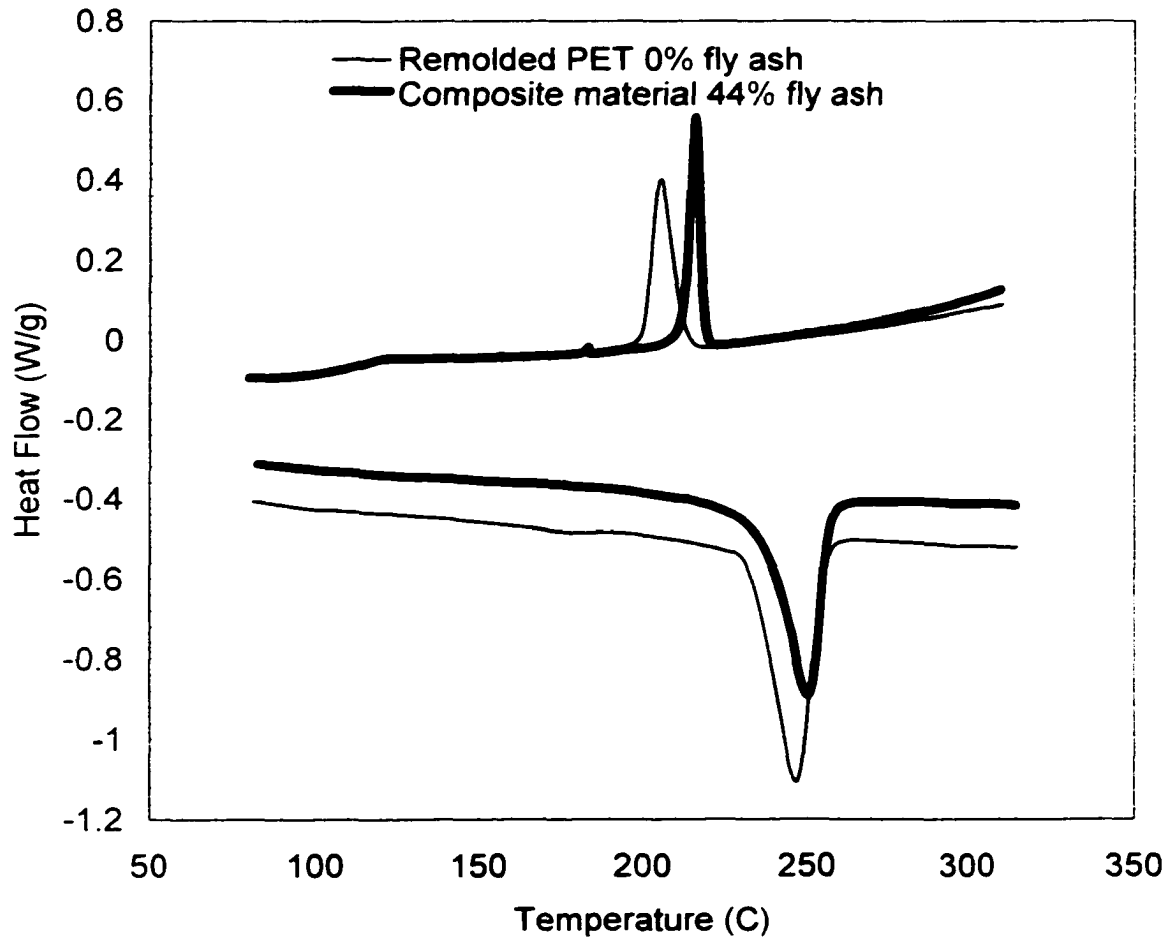


**Figure 9. DSC thermograms of remolded RPET and composite material with 44.4% fly ash content.**

## CHAPTER IV. SIMPLIFIED AND RAPID SOIL PERFORMANCE CLASSIFICATION SYSTEM

A paper to be submitted to the Geotechnical Testing Journal ASTM

David J. White<sup>1</sup> and Kenneth L. Bergeson<sup>1</sup>

**Abstract:** In response to recent evidence of poor highway embankment quality caused in part by improper soil identification and placement during construction, field-testing and laboratory analysis were conducted to develop a simple and rapid performance-based soil classification system that can be conducted in the field. Development of the Empirical Performance Classification (EPC) system is based on swell potential and frost susceptibility relationships derived from liquid limit, plasticity index, and fines content ( $\leq 75 \mu\text{m}$ ). From these parameters the EPC system is used to classify soils into one of three categories: select, suitable or unsuitable. This paper presents the background for the development of this system and procedures for its use. A field trial in Iowa indicates that Iowa Department of Transportation field personnel can effectively use the EPC system to classify soils in the field and to better link design with construction activities. Increased field soil classification is expected to improve long-term performance of cohesive earth embankments.

### Introduction

Soil volumetric stability as a function of swell potential and frost susceptibility is a notable engineering property that significantly affects the long-term performance of subgrade

---

<sup>1</sup> Pre-Doctoral Research Associate and Professor, respectively, Department of Civil and Construction Engineering, Iowa State University

soils and their capacity to support pavement structures. In the early 1900's engineering soil classification systems evolved from the need to group soils with similar volumetric stability and strength properties together for highway and airport construction (Terzaghi 1926, 1927, Hogentogler et al. 1931, Hogentogler and Willis 1934, Casagrande 1932, 1948). In 1927 Terzaghi reported that soil classification for engineering purposes should not be based solely on arbitrary data such as liquid limit or plasticity index or even textural classification, but rather the final system of soil classification should be based on the complex behavior of soil "under various conditions of stress and confinement". It was proposed that the following information be collected:

- Volume change produced by an external pressure (compressibility and elasticity)
- Speed with which volume change follows a change of pressure (coefficient of consolidation).
- Permeability
- Volume change due to drying and wetting (shrink/swell potential).
- Consistency in two extreme states (Atterberg limits). (Terzaghi 1927)

By evaluating these soil parameters, a well-defined prediction of soil performance is developed; however, testing equipment, cost and lengthy testing time limit the use of this process. In comparison with dam and levee construction, commercial building sites, and other sensitive projects, performing extensive laboratory analyses on the large quantities of soil used in highway embankment construction is not practical. As a result many highway agencies including the Iowa Department of Transportation (Iowa DOT) rely heavily on soil

classification methods based on soil plasticity in combination with grain-size distribution, soil density, pedologic information and soil origin in order to determine proper soil placement in the embankment. This process of soil classification has been shown to be relatively effective in identifying "unsuitable" expansive soils and frost prone silts for design, but it does not facilitate field identification (Bergeson et al. 1998). The current Iowa DOT classification process is limited by time-consuming test methods such as hydrometer analysis that is only performed in a permanent soil laboratory and requires a minimum of 24 to 48 hours before results are available. In Iowa an embankment project will average roughly 5,000-m<sup>3</sup> of excavation and placement per day. Therefore, a rapid method of soil classification that can be conducted in the field is vitally needed.

This paper presents an expedient and improved soil performance classification system for highway embankment construction termed the Empirical Performance Classification (EPC) system. The EPC system is intended for use by field personnel (i.e. inspectors and earthwork contractors). With this system soils classification can be conducted from the results of unsophisticated tests that can be rapidly performed in a field laboratory. A full-scale field trial has shown that the EPC system is a very efficient and practical method of classifying embankment soils and that it facilitates proper soil placement and provides a link between the soil design phase and construction phase.

The EPC system was derived from empirical relationships for liquid limit, plasticity index and fines content (percent passing the No. 200 sieve) that relate to soil swell potential and frost susceptibility. Furthermore, based on historical soils data collected in Iowa over the last 10 years, soil clay and silt fractions are shown to be strongly correlated to plasticity



index and fines content. Inherent in the usefulness of the EPC system is that soils with similar engineering properties are grouped together.

## **Background**

### *Soil Identification*

An investigation of newly constructed highway embankments was recently conducted in Iowa as a result of slope stability problems and rough pavements being observed shortly after embankments were paved and opened to traffic (Bergeson et al. 1998, White et al. 1999). These problems raised the question as to whether the current Iowa DOT soil identification and construction methods are adequate. Research began with an investigation of several embankments under construction. Initially, design engineers, field inspectors and earthwork contractors were interviewed to develop an understanding of the state-of-knowledge concerning proper soil identification, engineering soil properties, and desired embankment quality.

Foremost, it was observed that an understanding of soil identification procedures and proper placement within the embankment was lower than anticipated. Soils were being misidentified during construction in areas where the design borings were incomplete and when soils were mixed during the excavation, diking and compaction process. It became apparent that a link was missing between the design phase of the project (initial site borings) and the actual construction of the embankment. This problem was compounded by the fact that field personnel and contractors lack the equipment to perform soil classification testing in the field. However, even with the proper laboratory equipment, the current Iowa DOT soil classification procedures would require a lengthy and extensive laboratory analysis that lacks

efficiency. Table 1 summarizes the current Iowa classification procedure, which includes hydrometer analysis, carbon content determination, and Proctor density testing, as well as identification of soil origin (i.e. glacial till, residual) in order to classify a soil as “select”, “suitable”, or “unsuitable” for embankment construction. The disposal practices for unsuitable soils within the embankment are also presented.

As a result of not having the equipment or an efficient methodology to classify soils, field personnel rely heavily upon soil color, historical soil field names, and the observed soil’s capacity to support heavy construction equipment. Based solely on appearance, predicting the physical performance and judging the suitability of soils is difficult. “Red-dog”, “Tiger”, “Old-blue clay”, “Gumbo”, and “Sugar clay” are common field terms used to describe soils in Iowa and ultimately, to predict engineering performance. The names and properties of these field-described soils have been found to vary between earthwork contractors and Iowa DOT personnel and from region to region across the state (White et al. 1999). In situ testing on several completed embankment profiles supports the conclusion that soil identification based on the described historical soil names results in improper placement within the embankment, which leads to poor embankment quality.

### *In Situ Embankment Profiles*

Figures 1 and 2 show full depth profiles of liquid limit, plasticity index, moisture content, and soil classification of recently completed embankments constructed under the current Iowa DOT soil classification specification. In addition, relative swell potential, calculated from an empirical relation reported by Weston (1980), is shown. Figure 1 indicates that the embankment was constructed of mostly A-6 (CL) soils with some A-7-6

(CH) soils placed near the top of subgrade. Moisture contents ranged from 12.0 to 31.4 percent, liquid limit from 31 to 58, and plasticity index from 15 to 41. Most of the embankment profile was constructed of soil classified as A-6 (CL), which is generally considered a "suitable" subgrade soil. However, in the top 0.3 m of subgrade the swell potential is about 3 to 4 times higher than that in the underlying soils. This "unsuitable" material was misidentified by both the earthwork contractor and the Iowa DOT field personnel and should have been disposed of at least 1.5 m below subgrade elevation according to the Iowa DOT specified disposal practices. Reportedly, the earthwork contractor and Iowa DOT considered the A-7-6 (CH) soil as "select" based on the observation that when compacted and dried the soil became very hard and made an excellent haul road.

Figure 2 shows an embankment constructed at a different location with different Iowa DOT field personnel and contractor. The embankment profile consists of alternating layers of A-7-6 (CH) and A-4 (SC) with some A-2-4 (SM-SC) soils. For this embankment it appears as if the high swell potential soils (A-7-6) have been placed below the top of subgrade, but only to a depth of 0.5 m. At 0.5 m this "unsuitable" soil is within the zone of seasonal moisture change and lacks sufficient overburden confinement to maintain volumetric stability. Furthermore, the A-4 (SC) soils, which are typically rated as a moderate to high frost susceptible soil, should have been disposed of below the seasonal frost penetration depth to prevent heave and subsequent loss of bearing capacity during spring thaw. Neither of the described soils should have been used as "select" subgrade soil. These poor subgrade soils should have been altered by soil mixing, modified with fly ash or lime treatment, or replaced by hauling "select" from a different borrow pit. Misidentification or

lack of identification of expansive and frost prone soils is contributing to improper placement and will result in poor embankment performance. This will eventually lead to increased long-term pavement maintenance costs.

### **Development of the EPC System**

The development of the EPC system was initiated by dividing soils into two groups: (1) clayey soils and (2) silty soils. Clayey soils represent those materials that have both swell potential and frost susceptibility. Silty soils represent those materials that are only frost susceptible. In the following sections, the degree to which a clayey soil or a silty soil has swell potential or is frost susceptible is predicted from empirical data correlations for Iowa soils. These empirical relationships form the basis for the development of the EPC system.

#### *Clayey Soils*

One of the most deleterious engineering properties of a soil that contributes to pavement degradation is soil volume change. It is reported that damage costs from shrinking and swelling soils on buildings and pavement structures are greater than that produced by any other natural hazard including floods, hurricanes, tornadoes, and earthquakes (Krohn and Slosson 1980). Furthermore, it is estimated that damage from expansive soils in the United States reaches \$10 billion annually (Steinberg 1998). For highway embankment construction the best way to prevent costly pavement problems associated with expansive soils is through identification and proper disposal by selected placement within the embankment.

According to Mitchell (1993), swelling and shrinking of clayey soils is a function of clay content and mineralogy, which are strongly correlated to plasticity index and liquid

limit. Table 2 summarizes several correlations between swell potential and plasticity index, liquid limit and clay content. In order to relate clay content to plasticity index for Iowa soils, historical soil data collected over a 10-year period was analyzed. Figure 3 shows an empirical correlation for plasticity index versus clay content for the full range of Iowa soils. Clay content is estimated as

$$\% \text{ Clay-size fraction (by weight } < 2\mu\text{m)} = 0.95(\text{PI}) + 6.75 \quad (1)$$

where PI = plasticity index. As shown a strong correlation ( $\text{Adj. } R^2 = 0.89$ ,  $n = 12.045$ ) exists between plasticity index and clay content. This supports earlier findings that the average distribution of clay minerals in Iowa soils is relatively uniform with montmorillonite, illite, and kaolinite comprising 60, 30, and 10 percent, respectively (Russel and Haddock 1940). From Equation 1 it can be shown that Iowa soils with a plasticity index of 35 or higher contain approximately 40 percent and higher clay content, which is an indication of high to very high swell potential. A plasticity index of 10 or less indicates clay content of approximately 15 percent or less and is a boundary value for low swell potential. For the EPC system critical liquid limit values of 50 and plasticity index values of 10 and 35 were selected to develop the boundaries for the low to medium to high plasticity clays.

### *Silty Soils*

Preventing frost susceptible soils from being incorporated into the upper portion of the pavement subgrade is also a major component of the EPC system. Field pavement performance observations have shown that frost damage occurs if all of the following

conditions are present: (1) a supply of water, (2) freezing temperatures penetrating the ground, and (3) frost-susceptible soils. By eliminating one of these conditions frost damage is prevented. The most practical approach to prevent frost heave is to identify and eliminate frost susceptible soils from the subgrade. Frost penetration in Iowa ranges from 1.0 m in the south to 1.5 m in the north (Bowles 1985). Based on hydraulic principles such as soil permeability and capillary action, low plasticity clay and silts and fine sands are the most frost susceptible soils; whereas, gravels and heavy clays are the least susceptible. Table 3 summarizes several correlations between frost susceptibility and plasticity index, fines content and clay content.

To better define frost susceptible soils the Department of the Army (1983) developed empirical guidelines. From this investigation A-2-4, A-4, A-6 (ML, ML-OL, CL, CL-ML, and SM-SC) soils were found to have high to very high frost susceptibility with the silt fraction being the key variable. Identifying these silts and low to medium plasticity clays can eliminate the majority of frost susceptible soils from being incorporated into the subgrade. For Iowa soils the silt-size fraction can be estimated as

$$\% \text{ Silt-size fraction (by weight from 2 to } 75\mu\text{m)} = 0.984 (F_{200}) - 0.745 (\text{PI}) - 14.759 \quad (2)$$

where  $F_{200}$  = percent passing the No. 200 sieve. Figure 4 shows a strong correlation (Adj.  $R^2 = 0.92$ ,  $n = 12,045$ ) between the measured silt content and the estimated silt content from Equation 2. Well-graded silty or fine sandy Iowa soils with a plasticity index of 10 or less and fines content of 70 percent or greater are estimated to contain approximately 45 percent

silt content. In Iowa soils with 45 percent silt fraction and higher are considered highly frost susceptible and should not be placed directly under the pavement structure.

### **Empirical Performance Classification (EPC) System**

Table 4 and Figure 5 combine to form the EPC system, which can be used to determine the final soil classification for Iowa criteria. The EPC chart shown on Figure 5 was developed using the foregoing data to establish Atterberg limit boundaries for low to high plasticity clays. The boundary between clayey and silty soils is defined by the empirical Casagrande (1932) A-line, whereby clayey soils plot above the A-line and silty soils plot below the A-line. These empirical relationships form the basis for the EPC chart. The group index empirical formula (AASHTO 145-91) was used to establish the Fineness Designation Numbers (FDN) shown in the Iowa EPC criteria in Table 4, which is a means of weighting the effects of plasticity index, liquid limit, and percent passing the No. 200 sieve. As the group index decreases, the supporting capacity of the subgrade soil reportedly decreases. In the authors' opinion the group index also appears to be proportional to swell potential and inversely proportional to frost susceptibility. A group index of 15 indicates the transition from a "select" to a "suitable" soil for medium plasticity clays and a group index of 30 indicates the transition from a "suitable" to an "unsuitable" soil for high plasticity clays.

The information required for the EPC system includes the fines content (percent passing the No. 200 sieve) and plasticity characteristics of the minus No. 40 (425- $\mu\text{m}$ ) sieve material. The EPC chart (Fig. 5) is divided into preliminary soil groups, which are then used to determine the final soil classification as "select", "suitable", or "unsuitable".

“Select” soils are those placed directly under the pavement structure (0 to 0.6 m) to provide adequate volumetric stability, low frost potential, and good bearing capacity. “Suitable” soils underlie (0.6 to 1.5 m) the “select” soils and are usually in the zone of seasonal freeze/thaw and wetting and drying cycles. “Unsuitable” soils are commonly characterized as highly plastic clays or highly compressible, frost prone silts and are buried beneath the suitable soils (1.0 to 1.5 m below top of subgrade). By burying them, overburden stresses help to confine the soil and eliminate them from the zone of seasonal moisture change and frost penetration.

Several examples and comparison classifications between the EPC system and conventional soil index properties are shown in Table 5. The examples show how the required soil information (liquid limit, plasticity index, and percent passing the No. 200 sieve) can be reported.

### **EPC Procedure**

Initially a soil sample is obtained from the borrow pit during excavation or the grade during construction. Then index properties consisting of the liquid limit, plasticity index, and fines content (percent passing the No. 200 sieve) are determined. Once laboratory testing is complete the EPC system (Table 4 and Figure 5) is used to classify the soil as “select”, “suitable”, or “unsuitable” as described in the following steps:

1. Plot the liquid limit and plasticity index on the EPC chart (Fig. 5).
2. Determine in which designated preliminary soil group the soil plots, for example LL = 56 and PI = 37 plots in the region of high plasticity clay.



3. Determine if the fines content,  $F_{200}$ , is less than or greater than the Fineness Designation Number (FDN).
4. Classify soil "select", "suitable", or "unsuitable" based on guidelines shown in Table 4.

### **Classification Criteria**

In the following the liquid limit, plasticity index, and fines content for each preliminary soil group and the final soil classification are given for record. This information could be used to write a computer program for automation of the EPC system.

*High Plasticity Clays* – The soil is high plasticity clay if on Figure 5, the position of the plasticity index versus liquid limit plot falls on or above the A-line and the liquid limit is greater than 50.

1. Classify the soil as "suitable" if the percent by dry weight of the test specimen passing the No. 200 (75- $\mu$ m) sieve is less than the Fineness Designation Number.
2. Classify the soil as "unsuitable" if the percent by dry weight of the test specimen passes the No. 200 (75- $\mu$ m) sieve is more than the Fineness Designation Number.  
Dispose of the material at least 1.5 m below top of subgrade.

*Medium Plasticity Clays* – The soil is medium plasticity clay if the position of the plasticity index versus liquid limit plot falls on or above the A-line on Figure 5, and the

liquid limit falls on or below 50, and the  $PI \geq (28 - 0.38LL)$  when the liquid limit is from 28 to 38.

1. Classify the soil as “select” if the percent by dry weight of the test specimen passing the No. 200 (75- $\mu\text{m}$ ) sieve is less than the Fineness Designation Number.
2. Classify the soil as “suitable” if the percent by dry weight of the test specimen passing the No. 200 (75- $\mu\text{m}$ ) sieve is more than the Fineness Designation Number.

*Low/Medium Plasticity Clays* – The soil is low to medium plasticity clay if the position of the plasticity index versus liquid limit plot falls on or above the A-line, and the plasticity index falls on or above 10, and  $PI < (28 - 0.38LL)$  when the liquid limit is from 28 to 38.

1. Classify the soil as “select” if the percent by dry weight of the test specimen passing the No. 200 (75- $\mu\text{m}$ ) sieve is less than 60%.
2. Classify the soil as “suitable” if the percent by dry weight of the test specimen passing the No. 200 (75- $\mu\text{m}$ ) sieve is from 60% to 70%.
3. Classify the soil as “unsuitable” if the percent by dry weight of the test specimen passing the No. 200 (75- $\mu\text{m}$ ) sieve is more than 70%. Dispose of the material at least 1.0 m below top of subgrade.

*Low Plasticity Clays* – The soil is low plasticity clay if the position of the plasticity index versus liquid limit plot falls on or above the A-line, and the plasticity index falls below 10.

1. Classify the soil as “select” if the percent by dry weight of the test specimen passing the No. 200 (75- $\mu\text{m}$ ) sieve is less than or equal to 45% and the percent by dry weight of the test specimen passing the No. 40 (425- $\mu\text{m}$ ) sieve is less than or equal to 70%.
2. Classify the soil as “suitable” if the percent by dry weight of the test specimen passing the No. 200 (75- $\mu\text{m}$ ) sieve is from 46% to 70%.
3. Classify the soil as “unsuitable” if the percent by dry weight of the test specimen passing the No. 200 (75- $\mu\text{m}$ ) sieve is more than 70%. Dispose of the material at least 1.0 m below top of subgrade.

*Silts of Medium Compressibility* – The soil is a silt of medium compressibility if the position of the plasticity index versus liquid limit plot falls below the A-line, and the liquid limit is less than or equal to 50. Classify the soil as unsuitable. Dispose of the material at least 1.5 m below top of subgrade.

*Highly Compressible Silts and High Plasticity Organic Clays* – The soil is a highly compressible silt and high plasticity organic clay if the position of the plasticity index versus liquid limit plot falls below the A-line, and the liquid limit is greater than 50.

1. Classify the soil as “unsuitable” if the percent carbon by dry weight of the test specimen is equal or more than 3.0%. Use as slope dressing only.
2. Classify the soil as “unsuitable” if the percent carbon by dry weight of the test specimen is less than 3.0%. Dispose of the material within alternating layers of suitable material at least 1.5 m below top of subgrade.

### **Conclusions**

A new soil classification system was developed from empirical data correlations, which address anticipated field soil performance relative to swell potential and frost susceptibility. The Empirical Performance (EPC) system requires simple testing of Atterberg limits and determination of the amount of fines (percent passing the No. 200 sieve) in the soil for classification. These tests can be rapidly conducted in a field laboratory. The EPS system was developed to be used during soils design and construction phases and to provide a communication link between design and construction personnel on highway projects in order to improve embankment quality. This is expected to result in reduced long-term pavement maintenance costs.

Recently, the EPC system was used in Iowa on a highway pilot project to test feasibility. Research shows that the performance classification method is an effective tool to use when soils are being mixed during borrow excavation and construction processes or when soils are not identified on borrow pit boring logs. In order to perform the testing required on the pilot project, a field lab was equipped with an Atterberg limit test set, a microwave and scale, and No. 40 and 200 sieves. In addition, a water tank was furnished for sieve washing. Total testing time to perform one complete classification averaged one hour

for an efficient Iowa DOT technician. The EPC system is currently under review by the Iowa DOT for adoption and inclusion in statewide design and construction specifications.

### **Acknowledgements**

The Project Development Division of the Iowa Department of Transportation and the Iowa Highway Research Board sponsored this study under contract TR-401. The support of these agencies is greatly appreciated. The opinions, findings, and conclusions expressed in this paper are those of the authors and not necessarily those of the Iowa Department of Transportation.

### **References**

- Bergeson K., Jahren C., Wermager, M. and White, D., 1998. *Embankment Quality Phase I Report*. Project Development Division of the Iowa Department of Transportation and the Iowa Highway Research Board, Iowa DOT Project TR-401.
- Beskow, G., 1935. "Soil freezing and frost heaving with special application to roads and railways." *Swedish Geotechnical Society*, Series C, No. 375.
- Bowles, J., 1985. *Foundation Design*, McGraw-Hill Companies, Inc. New York.
- Casagrande, A., 1932. "Research on the Atterberg limits of soil." *Public Roads*, Vol. 13, No. 8, pp. 121-136.
- Casagrande, A. 1948. "Classification and identification of soils." *Transactions, ASCE*, No. 113, pp. 901-930.
- Chen, F.H., 1988. *Foundation on Expansive Soils*, American Elsevier Scientific Publication, New York.

- Department of the Army, 1985. *Pavement Design for Seasonal Frost Conditions*. TM 5-818-2. Washington.
- Fenton, T.E., 1995. "Prediction of Coefficient of Linear Extensibility Values for Iowa Soils." *Soil Survey Horizons*. Summer. pp. 55-59.
- Glossop, R. and Skempton, A.W., 1945. "Particle size in silts and sands." *Journal Inst. Civil Engineers*. Vol. 25. pp. 81-105.
- Hansbo, S., 1975 "Jordmatariallara." Amquist and Wiksell Forlag AB. Stockholm. pp. 218.
- Hogentogler, C.A., Wintermeyer, A.M. and Willis, E.A., 1931. "Subgrade soil constants. their significance and their application in practice." *Public Works*. Vol. 12, No. 4. pp. 89-108.
- Hogentogler, C.A., and Willis, E.A., 1934. "Subgrade soil testing methods." *Proceedings of American Society of Testing Materials*. No. 34, Part II.
- Holtz, W.G., and H.J. Gibbs, 1956. "Engineering Properties of Expansive Clays." *Transactions ASCE*. Vol. 121. pp. 641-677.
- Krebs, R.D. and Walker, E.D., 1971. *Highway Materials*. McGraw-Hill Companies, Inc., New York.
- Krohn, J.P. and Slosson, J.E., 1980. "Assessment of Expansive Soils in the United States." *Fourth International Conference on Expansive Soils*, Vol. 1. Denver.
- Mitchell, J.K., 1993, *Fundamentals of Soil Behavior*, Second Edition. John Wiley & Sons, Inc., New York.
- Russell, M.B. and Haddock, J.L., 1940. "The identification of clay minerals in five Iowa soils by the thermal methods." *Soil Sc. Soc. Am. Proc.* No. 5, pp. 90-94.

- Seed, H.B., Woodward, R.J., and Lundgran, R., 1962, "Prediction of swelling potential of compacted clays." *Proc. ASCE Journal of Soil Mechanics and Foundation Division*. Vol. 88, pp. 107-131.
- Steinberg, M., 1998. *Geomembranes and the Control of Expansive Soils in Construction*. McGraw-Hill, New York.
- Terzaghi, C., 1926. "Simplified soil tests for subgrades and their physical significance." *Public Works*, Vol. 7, No. 8, pp. 153-170.
- Terzaghi, C., 1927, "Principles of final soil classification." *Public Roads*, Vol. 8, No. 3, pp. 41-53.
- Weston, D.J., 1980. "Expansive Roadbed Treatment for Southern Africa." *Proceedings. Fourth Intonation Conference on Expansive Soils*, Vol. 1 pp. 339-360.
- White, D.J., Bergeson, K.L., Jahren, C.T., Wermager, M., 1999. *Embankment Quality Phase II Report*, Project Development Division of the Iowa Department of transportation and the Iowa Highway Research Board, Iowa DOT Project TR-401.

TABLE 1—Current Iowa DOT specification for cohesive soil classification into “select”, “suitable”, and “unsuitable” categories

Select soils (must meet all conditions - typically used in top 0.6 m of subgrade)	Suitable soils (must meet all conditions - used throughout fill except for top 0.6 m of subgrade)	Unsuitable soils (Requirements for use at different depths)
<ul style="list-style-type: none"> <li>• 45 percent or less silt size fraction (0.075-0.002 mm)</li> </ul>	<ul style="list-style-type: none"> <li>• 1500 kg/m<sup>3</sup> or greater density (AASHTO T 99 Proctor density)</li> </ul>	<ul style="list-style-type: none"> <li>• Slope dressing only               <ul style="list-style-type: none"> <li>- peat or muck</li> <li>- soil with plastic limit <math>\geq 35</math></li> <li>- A-7-5 or A-5 having density &lt; 1350 kg/m<sup>3</sup></li> </ul> </li> </ul>
<ul style="list-style-type: none"> <li>• 1750 kg/m<sup>3</sup> or greater density (AASHTO T99 Proctor density)</li> </ul>	<ul style="list-style-type: none"> <li>• Group Index &lt; 30 (AASHTO M 145-90)</li> </ul>	<ul style="list-style-type: none"> <li>• Disposal 1 m below top of subgrade               <ul style="list-style-type: none"> <li>- All soils other than A-7-5 or A-5 having density &lt; 1500 kg/m<sup>3</sup></li> <li>- All soils other than A-7-5 or A-5 containing <math>\geq 3.0\%</math> carbon</li> </ul> </li> </ul>
<ul style="list-style-type: none"> <li>• Plasticity index &gt; 10</li> </ul>		<ul style="list-style-type: none"> <li>• Disposal 1 m below top of subgrade               <ul style="list-style-type: none"> <li>- A-7-6 (30 Or greater)</li> <li>- Residual clays overlying bedrock regardless of classification</li> </ul> </li> </ul>
<ul style="list-style-type: none"> <li>• A-6 or A-7-6 soils of glacial origin</li> </ul>		<ul style="list-style-type: none"> <li>• Disposal 1.5 m below top of subgrade with alternate layers of suitable soils               <ul style="list-style-type: none"> <li>- shale</li> <li>- A-7-5 or A-5 soils having density from 1350 kg/m<sup>3</sup> to 1500 kg/m<sup>3</sup></li> </ul> </li> </ul>



TABLE 2—*Relationships between swell potential and soil index properties*

Reference	Index Criteria		Potential for Expansion
Seed et al. (1962)	PI < 15		Low
	10 ≤ PI ≤ 30		Medium
	20 ≤ PI ≤ 55		High
	PI > 40		Very High
Department of the Army (1983)	LL < 50	PI < 25	Low
	50 ≤ LL ≤ 60	25 ≤ PI ≤ 35	Medium
	LL > 60	PI > 35	High
Krebs and Walker (1971)	PI < 15		Low
	15 ≤ PI ≤ 24		Medium
	25 ≤ PI ≤ 46		High
	PI > 46		Very High
Holtz and Gibbs (1956)	PI < 18		Low
	15 ≤ PI ≤ 28		Medium
	25 ≤ PI ≤ 41		High
	PI > 35		Very High
Chen (1988)	F <sub>200</sub> < 30	LL < 10	Low
	30 ≤ F <sub>200</sub> ≤ 60	40 ≤ LL ≤ 60	Medium
	60 ≤ F <sub>200</sub> ≤ 95	30 ≤ LL ≤ 40	High
	F <sub>200</sub> > 35	LL > 60	Very High
Fenton (1995)	CC < 25		Low
	25 ≤ CC ≤ 35		Moderate
	36 ≤ CC ≤ 45		High
	CC > 45		Very High

Note: LL = liquid limit; PI = plasticity index; F<sub>200</sub> = percent passing 75 μm (No. 200) sieve; CC = clay content for Iowa soils (< 2 μm).

TABLE 3—*Relationships between frost susceptibility and soil index properties*

Reference	Index Criteria	Comments
Transport and Road Research Laboratory (1970)	PI < 20	Frost Susceptible
	PI > 20	Non-Frost Susceptible
Beskow (1935)	F <sub>200</sub> > 70	Frost-heaving glacial soils
Glossop and Skempton (1945)	Silt size < 30	Non-frost heaving well-sorted soil
Hansbo (1975)	CC 15-25%	Strong frost susceptibility
	CC > 40% and Fines > 16%	Moderate frost susceptibility

Note: PI = plasticity index; F<sub>200</sub> = percent passing 75 μm (No. 200) sieve; CC = clay content (< 2 μm), fines = 0.06mm.

TABLE 4—Iowa EPC criteria for cohesive soils.

Preliminary Soil Group	Final Classification and Criteria			Unsuitable Disposal Requirements (placement below top of subgrade)
	Select	Suitable	Unsuitable	
Low plasticity clays	$F_{200} \leq 45$ and $F_{40} \leq 70$	$46 \leq F_{200} \leq 70$	$F_{200} > 70$	1.0 m
Low/Medium plasticity clays	$F_{200} < 60$	$60 \leq F_{200} \leq 70$	$F_{200} > 70$	1.0 m
Medium plasticity clays	$F_{200} \leq \text{FDN}$	$F_{200} > \text{FDN}$	—	—
High plasticity clays	—	$F_{200} \leq \text{FDN}$	$F_{200} > \text{FDN}$	1.5 m
Silts of medium compressibility	—	—	All soils in this region	1.5 m
Highly compressible silts and high plasticity organic clays	—	—	All soil in this region	<ul style="list-style-type: none"> <li>• Dispose within alternating layers of suitable material at least 1.5 m</li> <li>• Slope dressing only if carbon content <math>\geq 3.0\%</math></li> </ul>

NOTE:  $F_{200}$  = Percent passing 75  $\mu\text{m}$  (No. 200) sieve;  $F_{40}$  = percent passing 425  $\mu\text{m}$  (No. 40) sieve; FDN = Fineness Designation Numbers from Fig. 5.

TABLE 5—Comparisons of Empirical Performance Classification with the AASHTO and Unified classification systems

NO.	LL	PI	Percent passing No. 40 sieve	Percent passing No. 200 sieve	AASHTO Classification System (Group Index)	Unified Classification System Group Symbol	Preliminary Descriptive Regions for Cohesive Soils from Fig. 3	Empirical Performance Classification
1	28	4	—	39	A-4(1)	ML	Inorganic Silts of Medium Compressibility	Unsuitable
2	22	9	68	44	A-4(0)	CL-ML	Low Plasticity Clays	Select
3	19	7	—	63	A-4(0)	CL-ML	Low Plasticity Clays	Suitable
4	33	11	—	62	A-6(7)	CL	Low/Medium Plasticity Clays	Suitable
5	35	21	—	61	A-6(10)	CL	Medium Plasticity Clays	Select
6	49	27	—	95	A-7-6(28)	CL	Medium Plasticity Clays	Suitable
7	57	41	—	74	A-7-6(29)	CH	High Plasticity Clays	Suitable
8	63	36	—	84	A-7-6(36)	CH	High Plasticity Clays	Unsuitable
9	63	45	—	94	A-7-5(33)	MH	High Plasticity Clays	Unsuitable
10	65	41	—	71	A-7-6(29)	CH	High Plasticity Clays	Suitable
11	76	37	—	91	A-7-5(42)	MH	Highly compressible inorganic silts and high plasticity clays	Unsuitable
12	97	71	—	95	A-7-6(81)	CH	High Plasticity Clays	Unsuitable

Note: Percent passing the No. 40 sieve is only required for soils that plot in the Low plasticity clay region as indicated on Fig. 5 and have less than 46 percent passing the No. 200 sieve

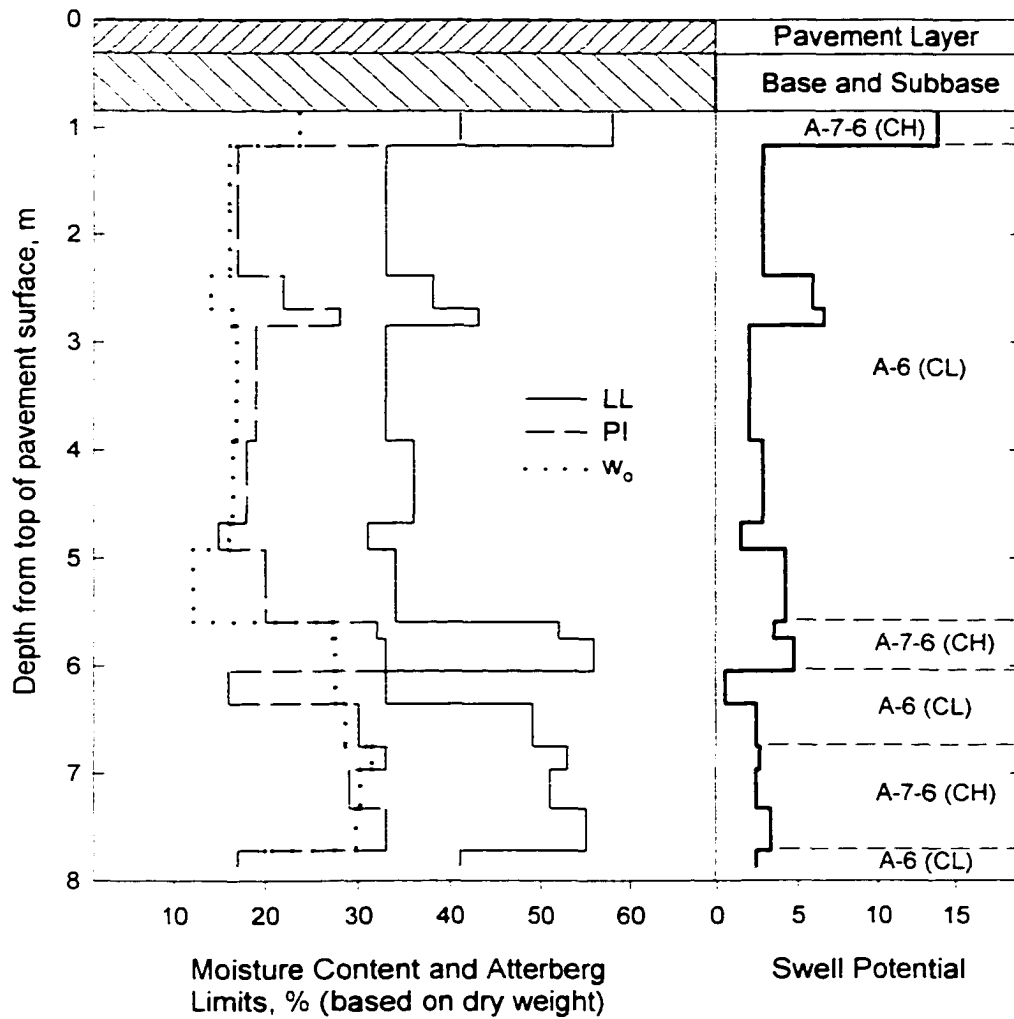


FIG 1 - Swell potential of recently constructed cohesive embankment based on empirical relationship from Weston (1980)  $SP = 0.00411(LL_w)^{4.17}q^{-0.386}w_o^{-2.33}$ .

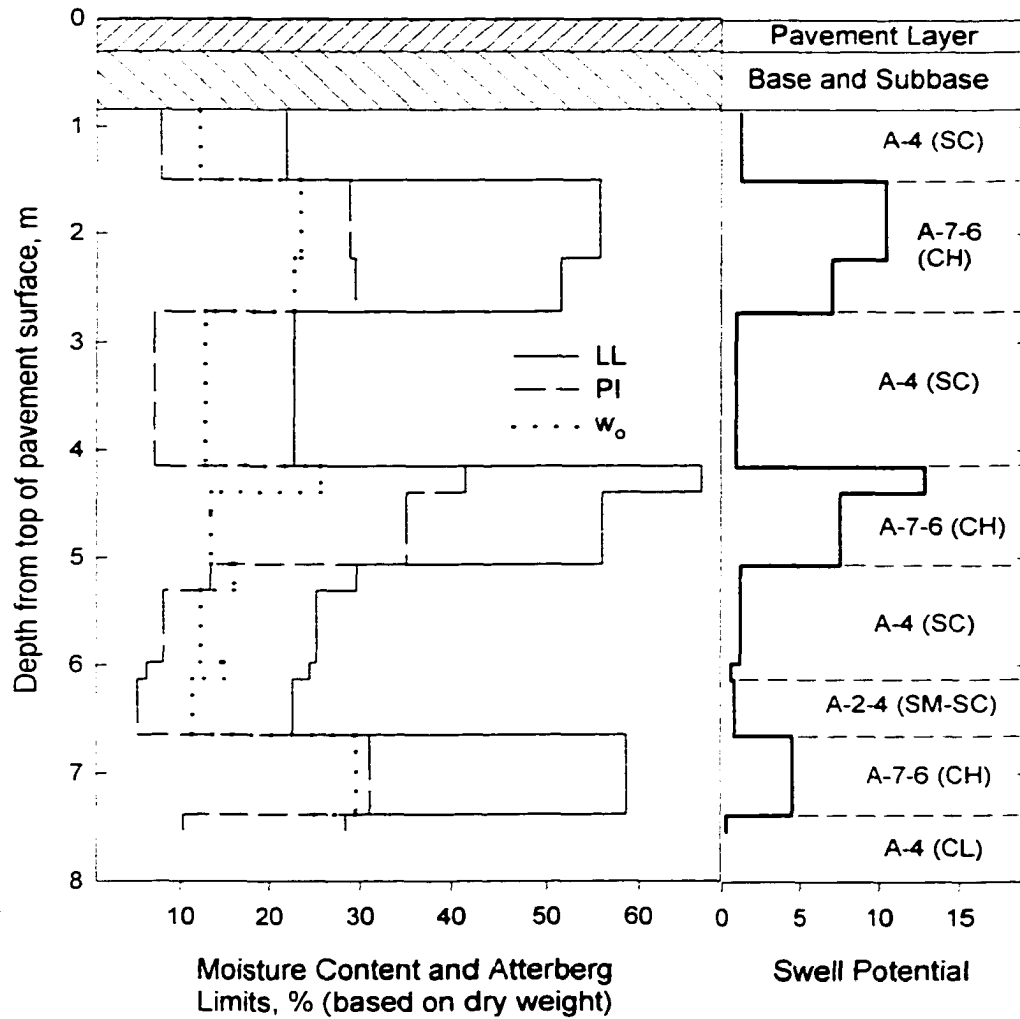


FIG 2 - Swell potential of recently constructed cohesive embankment based on empirical relationship from Weston (1980)  $SP = 0.00411(LL_w)^{4.17} q^{-0.386} w_0^{-2.33}$

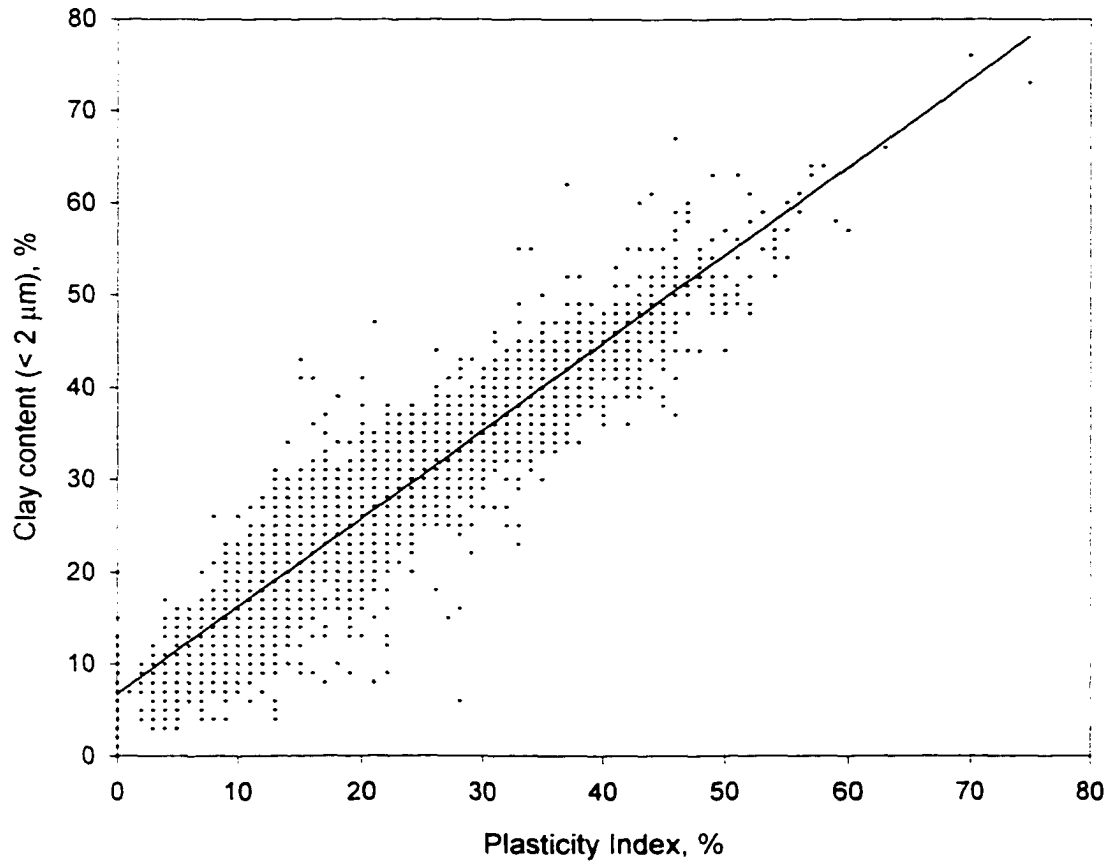
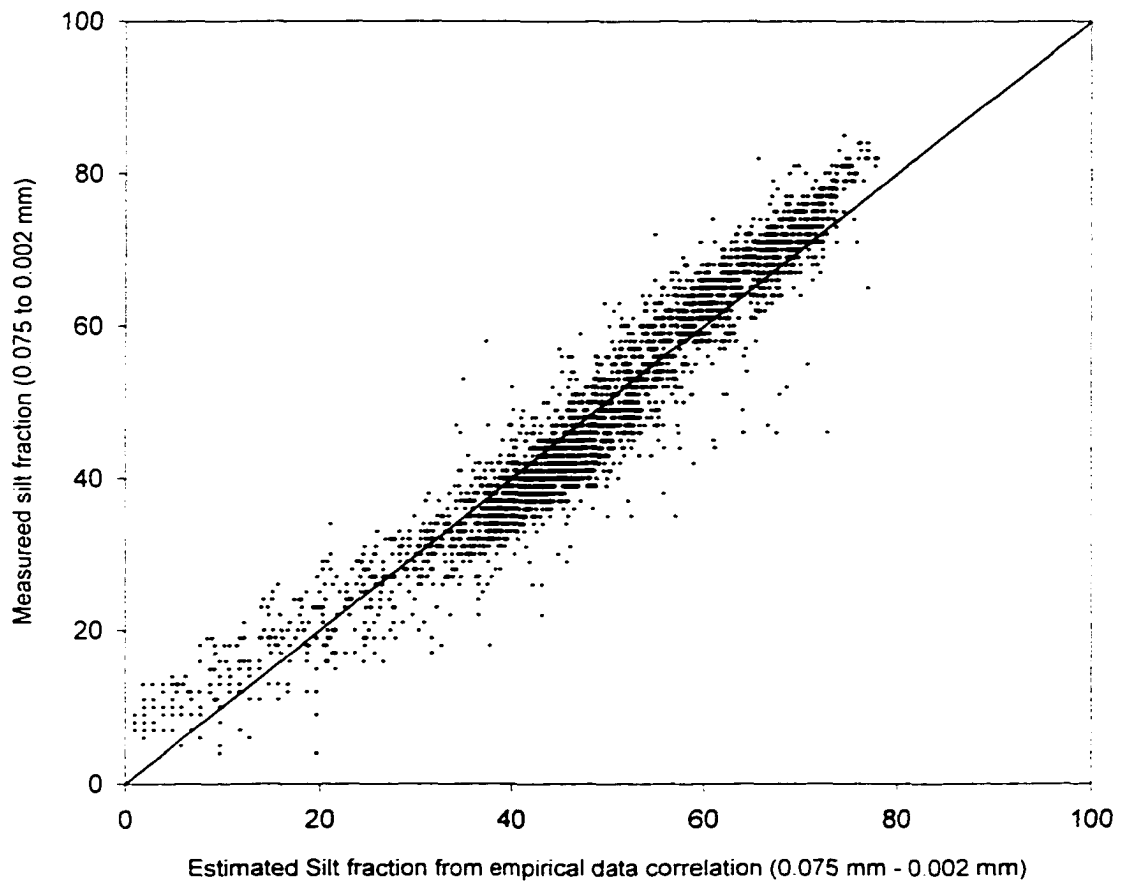


FIG 3 - Relationship between clay content and plasticity index for Iowa soils



*FIG 4-Relationship between measured silt content and predicted silt content from empirical data correlation based on plasticity index and fines content for Iowa soils*



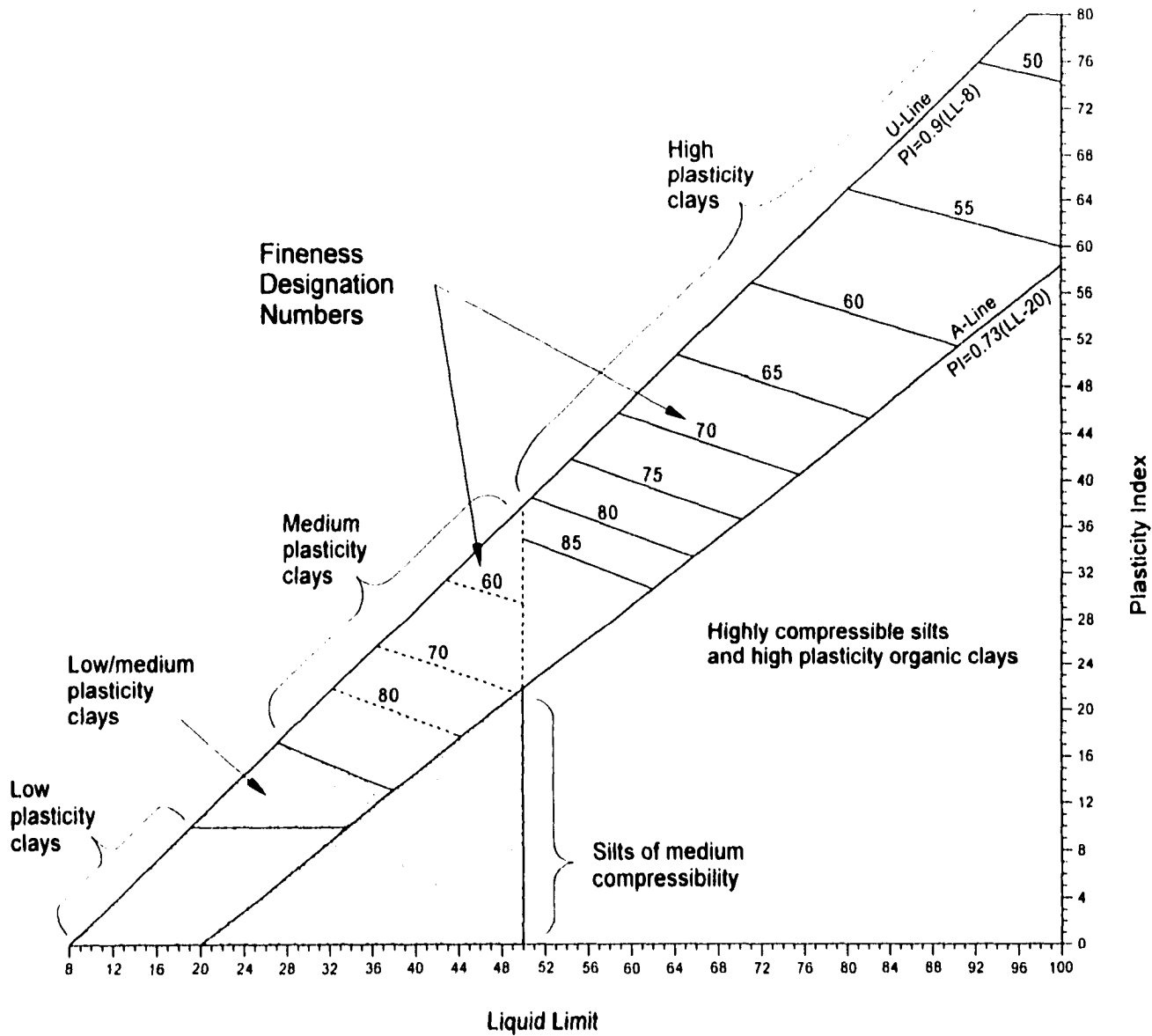


FIG 5 - Empirical Performance Classification (EPC) chart

## CHAPTER V. GENERAL CONCLUSIONS

The major conclusions derived from this research are summarized separately for each paper as follows:

### **Long Term Strength and Durability of Hydrated Fly Ash Road Bases**

- The strength properties and environmental benefits of using reclaimed HFA make it a desirable road base material from an engineering, environmental, and economic perspective. In comparison with full depth portland cement concrete (PCC) or asphaltic cement concrete (ACC) in combination with aggregate base materials, pavement costs can be reduced by up to 50 percent by using a thin asphaltic concrete surface course in combination with the described calcium activated HFA base material.
- HFA material is unique in that if water is available for hydration, long-term pozzolanic reactions increase strength with time. Long-term strength gain was evidenced in the laboratory and from extracted core samples.
- Despite delamination occurring in the AFBC activated HFA test section, it has been performing very well under heavy traffic loads through 5 years. However, in the authors' opinion activators containing high levels of sulfates should be avoided in the future.
- Future materials analysis (x-ray and thermal analysis) of HFA bases should focus on long-term reaction product formation with emphasis on ettringite and thaumasite

formation and on the possibility that because the HFA aggregate is rich in silica that alkali-silica gel is forming and causing the observed delamination.

### **Microstructure of Composite Material from High-Lime Fly Ash and RPET**

- An innovative composite material has been developed from high-lime fly ash and recycled polyethylene terephthalate (PET), which can potentially be used as a construction building material. Primary uses for this material are anticipated to include construction panels, masonry units and polymer aggregate concrete materials.
- Municipalities, landfill companies, and power generating stations will benefit from production of this composite material because of reduced landfill space requirements. In addition, consumers and manufacturers will benefit from an expanded product line. Therefore, it is concluded that this will be a favorable technology both environmentally and economically.
- Future testing should include evaluation for specific building material applications. Currently, research is underway to evaluate the resistance of the composite material to sulfuric acid attack and ultraviolet light degradation.

### **Simplified and Rapid Soil Performance Classification System**

- The EPC system is a new soil classification system for grouping soils together by predicting soil performance based on swell potential and frost susceptibility

relationships. These relationships are derived from published literature and empirical correlations developed for clay and silt content for Iowa soils.

- This system is intended to increase field soil identification and to better link design with construction activities, which will reduce long-term pavement maintenance costs.
- In the future a full-scale evaluation of the EPC system is planned on an Iowa Department of Transportation embankment project. This pilot project will be used to make adjustments to the EPC system if needed.

## **GENERAL ACKNOWLEDGEMENT**

The author extends sincere thanks to the Iowa Department of Transportation (DOT), the Iowa Fly Ash Affiliates Research Program, and the American Coal Ash Association (ACAA) for funding these research projects.

The writer would like to express his gratitude to everyone who has provided assistance and guidance throughout the course of this research. Foremost, Dr. John Pitt and Dr. Kenneth L. Bergeson are thanked for their assistance and advice during the course of his academic career. Grateful thanks are extended to the members of the committee, Dr. R.L. Handy, Dr. Brian Coree, Dr. Charles Jahren, and Dr. Igor Beresnev for their guidance. Also, the help of Mr. Aaron Gaul and Mr. Mark Seidl is greatly appreciated. Finally, much appreciation is extended to Ms. Jennifer Dvorak for her thoughtful support, patience, and understanding.